AD A088752

DDC FILE COPY

Unclassified REPORT DOCUMENTATION PAGE LEVEL II

READ INSTRUCTIONS BEFORE COMPLETING FORM

1. REPORT NUMBER: AFOSR-TR- 80-0695
2. GOVT ACCESSION NO.: AD-A088 752
3. RECIPIENT'S CATALOG NUMBER:

4. TITLE (and subtitle): SURFACE WAVES, SEISMIC REFRACTION AND UPPER MANTLE STRUCTURE OF THE BASIN AND RANGE

5. TYPE OF REPORT & PERIOD COVERED: Semiannual technical, April 1, 1979 to Sept. 30,

6. PERFORMING ORG. REPORT NUMBER:

7. AUTHOR(s): Keith F. Priestley

8. CONTRACT OR GRANT NUMBER(s): F49620-77-C-0070

9. PERFORMING ORGANIZATION NAME AND ADDRESS:
Institute of Geophysics and Planetary Physics
Scripps Institution of Oceanography, UCSD
La Jolla, California 92093

10. PROGRAM ELEMENT, PROJECT, TASK AREA & WORK UNIT NUMBERS:
A.O. 3291-31
OD60

11. CONTROLLING OFFICE NAME AND ADDRESS:
Advanced Research Projects Agency
1400 Wilson Blvd.
Arlington, VA 22209

12. REPORT DATE: January 20, 1980

13. NUMBER OF PAGES: 50

14. MONITORING AGENCY NAME & ADDRESS (if different from Controlling Office):
Air Force Office of Scientific Research/NP
Bolling Air Force Base
Washington, D. C. 20332

15. SECURITY CLASS. (of this report): Unclass.

15a. DECLASSIFICATION DOWNGRADING SCHEDULE:

16. DISTRIBUTION STATEMENT (of this Report):

Approved for public release; distribution unlimited.

17. DISTRIBUTION STATEMENT (of the abstract entered in Block 20, if different from Report):

DTIC ELECTE SEP 5 1980 D

18. SUPPLEMENTARY NOTES:

19. KEY WORDS (Continue on reverse side if necessary and identify by block number):

Surface wave dispersion, refraction, Basin and Range, mantle structure

20. ABSTRACT (Continue on reverse side if necessary and identify by block number):

Earlier study of Great Basin structure using surface waves have been extended to include the Southern Basin and Range of Arizona, and the Volcanic Plateau of Northern Nevada and Southern Oregon. The crust of the Southern Basin and Range is slightly thinner than that of the Great Basin while the mantle structure is similar. The Volcanic Plateau has a thicker crust (based on refraction data) than the Great Basin while the mantle lid zone is either thin or absent.

DD FORM 1 JAN 73 1473 EDITION OF 1 NOV 65 IS OBSOLETE

UNCLASSIFIED
SECURITY CLASSIFICATION OF THIS PAGE (When Data Entered)

(18) AFOSR-TR-(19) 80-0695

UNIVERSITY OF CALIFORNIA, SAN DIEGO

BERKELEY • DAVIS • IRVINE • LOS ANGELES • RIVERSIDE • SAN DIEGO • SAN FRANCISCO — SANTA BARBARA • SANTA CRUZ

INSTITUTE OF GEOPHYSICS AND
PLANETARY PHYSICS
LA JOLLA LABORATORIES A-025
SCRIPPS INSTITUTION OF OCEANOGRAPHY

LA JOLLA, CALIFORNIA 92093

(11) 20 Jan 80

(12) 32

SEMIANNUAL
TECHNICAL REPORT NO. 4
20 JANUARY 1980

ARPA Order No.	3291
Program Code	TF10-7F10
Name of Contractor	University of Nevada, Reno
Effective Date of Contract	01 February 1977
Contract Expiration Date	30 September 1980
Amount of Contract Dollars	$138,084
Contract Number	(15) F49620-77-C-0070, ARPA Order No-3291
Principal Investigator	(10) Keith F. Priestley, 702-784-4975
Program Manager	Keith F. Priestley
Short Title of Work	(6) SURFACE WAVES, SEISMIC REFRACTION AND UPPER MANTLE STRUCTURE OF THE BASIN AND RANGE

(9) Semiannual technical report no. 4.
1 Apr-30 Sep 79,

Sponsored by
Advanced Research Projects Agency (DOD)
ARPA Order No. 3291
Monitored by AFOSR Under Contract # F49260-77-C-0070

Technical Report Summary

In an earlier paper (Priestley and Brune, 1978) we proposed a shear wave model for the Great Basin of Nevada and Western Utah based on the analysis of seismic surface waves. We have now nearly completed a similar study for the Basin and Range of Arizona and Southern Nevada, and for the Volcanic Rift province of Northern Nevada, Eastern Oregon and Washington, and Southwest Idaho. The phase velocities at long periods (~40 sec) are low in each of these areas similar to the Great Basin. This indicates a uniform presence of a low velocity zone for shear waves throughout much of Western North America. All of our observed phase velocities are lower than those observed by Biswas and Knopoff (1974) for Western North America. In particular, our observations in the Great Basin and Volcanic Rift provinces are .10 - .20 k/s lower than Biswas and Knopoff (1974) reported for the path GSC-LON. We have only been able to resolve this by assuming the single South American event they studied for this path was affected by lateral refraction.

We have completed our study of S_n propagation in the Great Basin. The data was analyzed in terms of both a superposition of normal modes and interfering body waves. We conclude that while this phase places constraints on the upper mantle shear wave velocity, it does not significantly constrain the mantle lid thickness.

Research Efforts

A. Great Basin - (See Appendix A)

B. Southern Basin and Range

Data from three long period stations (TNP, TUC, GSC--Figure 1) were studied to determine a shear wave model for the Basin and Range of Southern Nevada and Arizona. Additional surface wave data from the Lawrence Livermore Laboratory seismic stations (KNB, LAC, and MNV) and LRSM seismic stations (CP-CL, KN-UT, and MN-NV) are being analyzed to examine the crustal structure in the transition zone between the Great Basin and the Southern Basin and Range. There is marked contrast between the characteristics of the Northern Basin and Range (the Great Basin) and the Southern Basin and Range. The Great Basin is characterized by high seismicity, recent faulting, high heat flow, elevated topography and recent volcanism. In contrast, the Basin and Range of Arizona is characterized by a low level of seismic activity, a lack of recent faulting, subdued topography and an older age of volcanism. These differences presumably indicate that the Basin and Range structure of Arizona predates that of the Great Basin and together they show a continuing evolutionary process.

Figures 2 and 3 show observed fundamental mode Love and Rayleigh wave phase velocities observed for the Southern Basin and Range. At long periods, these are similar to that previously observed for the Great Basin indicating the presence of a broad low velocity zone for shear

waves similar to that proposed for the Great Basin. The higher phase velocities observed at shorter periods (<40 sec) indicate a somewhat thinner crust within the Southern Basin and Range compared to the Great Basin. This has previously been noted by Bache et al. (1978).

C. Volcanic Rift Province

Data from six long period seismograph stations (LON, BOI, LOG, DUG, REN, KFO--Figure 1) surrounding the Volcanic Rift province were studied to determine a shear wave model for this area. The region was studied as a whole, and the subregion consisting of the Western Snake River Plain was analyzed as a separate tectonic unit. These results are summarized in Figures 4 and 5. Fundamental mode Rayleigh wave phase velocities for the Volcanic Rift province are compared with that observed for the Great Basin in Figure 6. The Volcanic Rift dispersion differs only slightly from that observed for the Great Basin. However, the observed dispersion for the Western Snake River Plain is significantly lower.

Figure 7 compares an average Great Basin crustal with two proposed crustal models for the Snake River Plain. Using these crustal models as control we have varied the upper mantle shear wave structure to fit the observed dispersion (Figure 8). In comparison with the Great Basin, the Western Snake River Plain has a slightly thicker crust (40 km vs. 35 km) and a much thinner upper mantle lid. The data requires a thinning of the lid to approximately 10 km and a lowering of the shear wave velocity from 4.5 k/s to 4.3 k/s. Within the scatter of the data, the lid zone may be absent. This thinner lithosphere proposed for the Western Snake River Plain is consistent with observed heat flow.

REFERENCES

Bache, T., W. Rodi, and D. Harkrider (1978). Crustal structure inferred from Rayleigh-wave signatures of NTS explosions, B.S.S.A., 68, 1399-1414.

Biswas, N. N. and L. Knopoff (1974). The structure of the upper mantle under the United States from the dispersion of Rayleigh waves, Geophys. J. Roy. Astron. Soc., 36, 515-539.

Hill, D., and L. Pakiser (1966). Crustal structure between Nevada Test Site and Boise, Idaho, in The Earth Beneath the Continents: Am. Geophys. Union, Geophys. Mono. 10, 391.

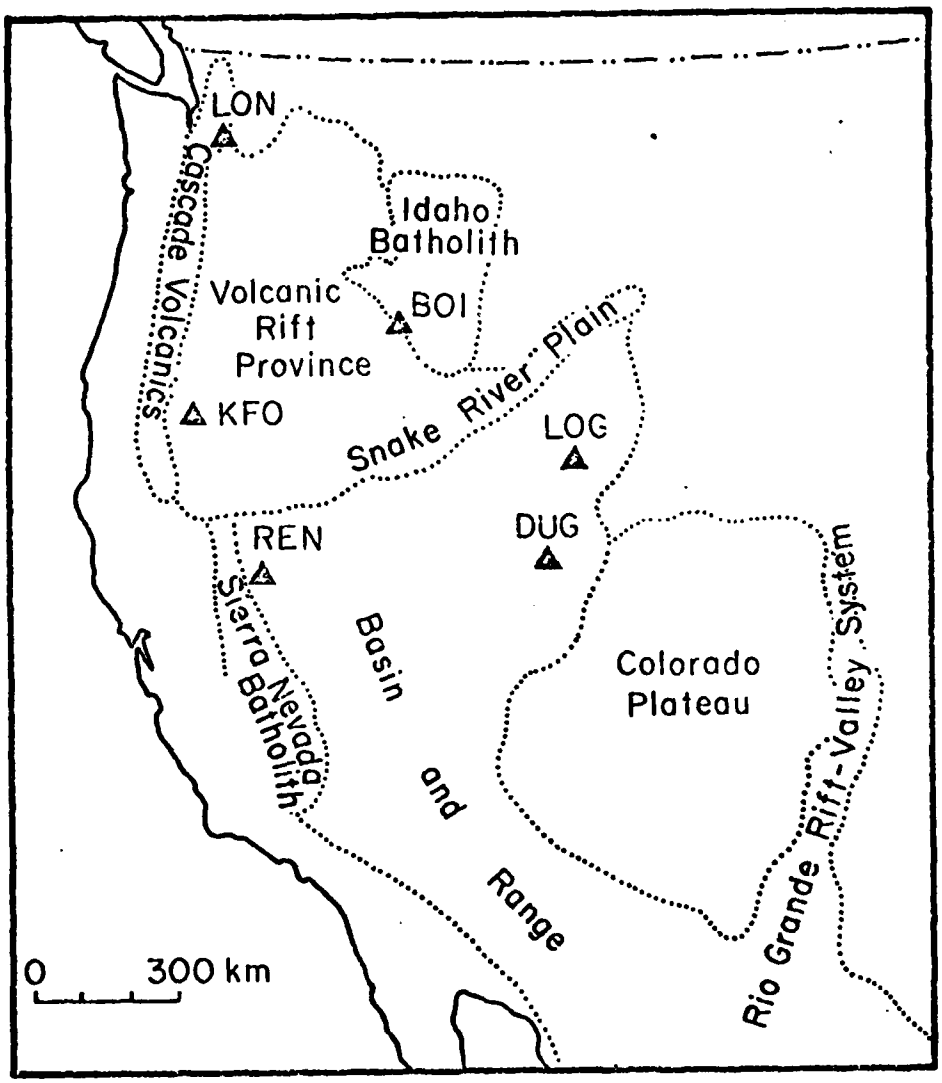
LON
Cascade Volcanics
Idaho Batholith
Volcanic Rift Province
BOI
KFO
Snake River Plain
LOG
DUG
REN
Sierra Nevada Batholith
Basin and Range
Colorado Plateau
Rio Grande Rift-Valley System
0
300 km

Figure 1

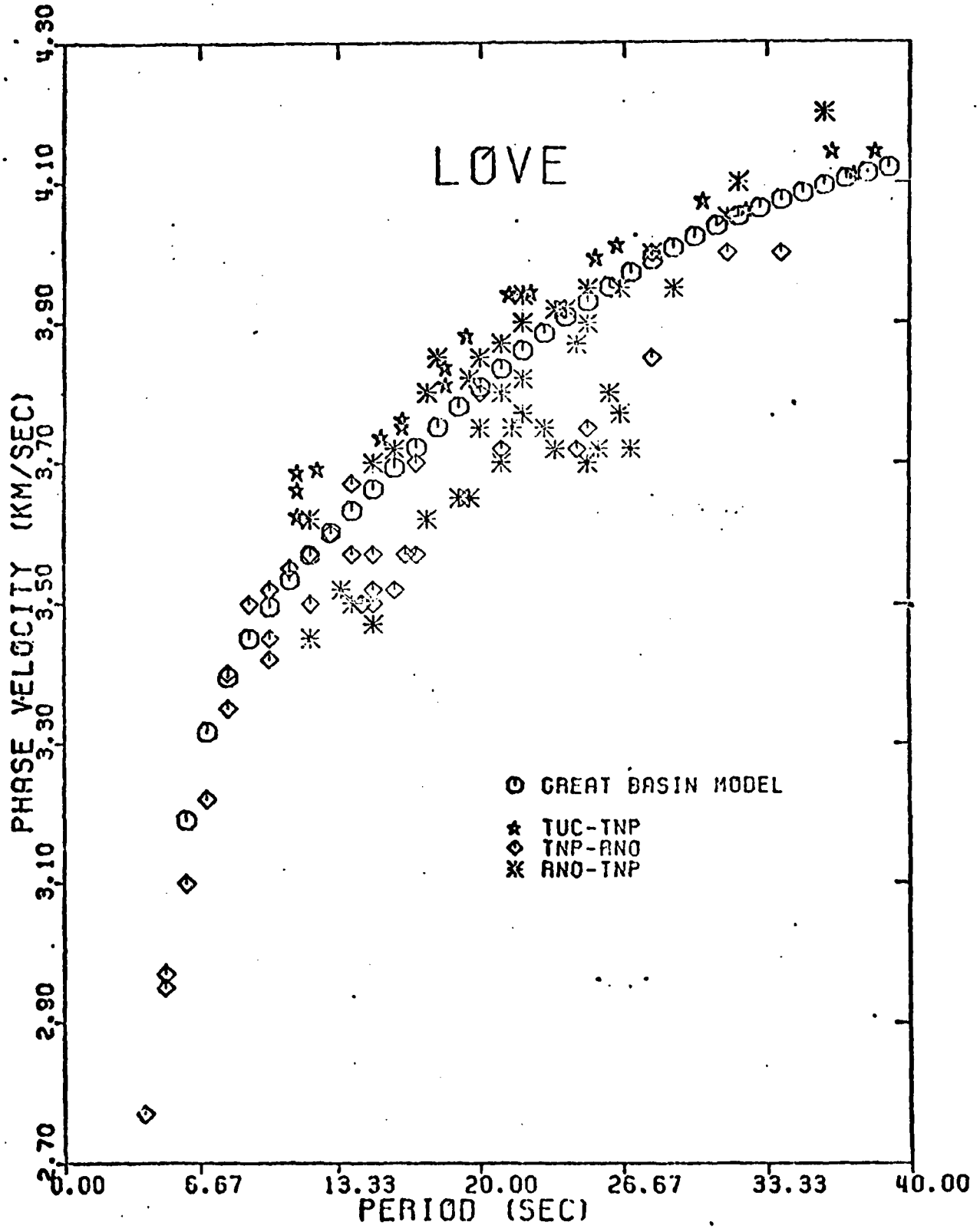
LOVE
PHASE VELOCITY (KM/SEC)
2.70
2.90
3.10
3.30
3.50
3.70
3.90
4.10
4.30
0.00
6.67
13.33
20.00
26.67
33.33
40.00
PERIOD (SEC)
GREAT BASIN MODEL
TUC-TNP
TNP-ANO
ANO-TNP

Figure 2

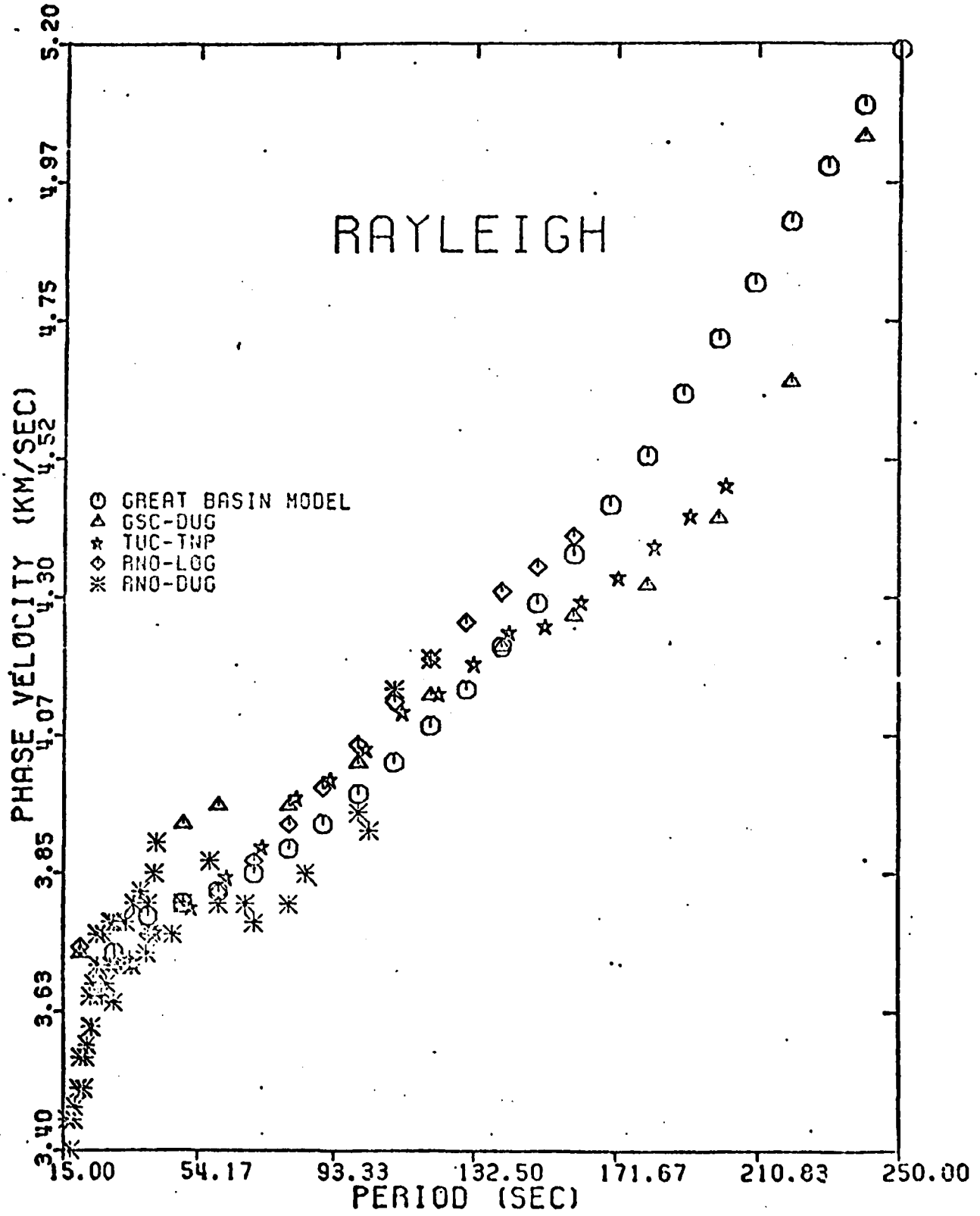
RAYLEIGH
GREAT BASIN MODEL
GSC-DUG
TUC-TNP
RNO-LOG
RNO-DUG
PHASE VELOCITY (KM/SEC)
5.20
4.97
4.75
4.52
4.30
4.07
3.85
3.63
3.40
15.00
54.17
93.33
132.50
171.67
210.83
250.00
PERIOD (SEC)

Figure 3

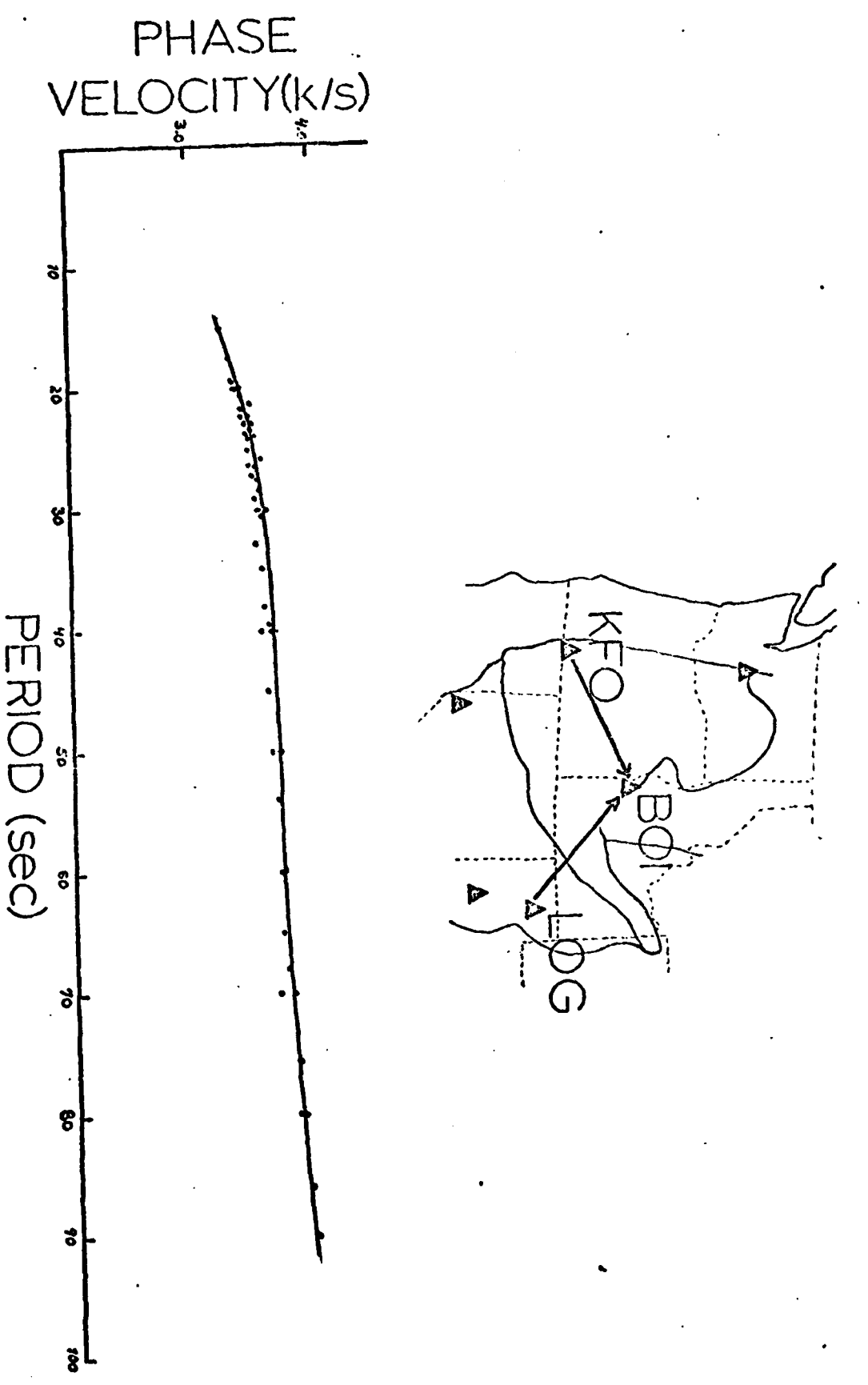
PHASE
VELOCITY(k/s)
3.0
4.0
10
20
30
40
50
60
70
80
90
100
PERIOD (sec)
KFO
BOI
LOG

Figure 4

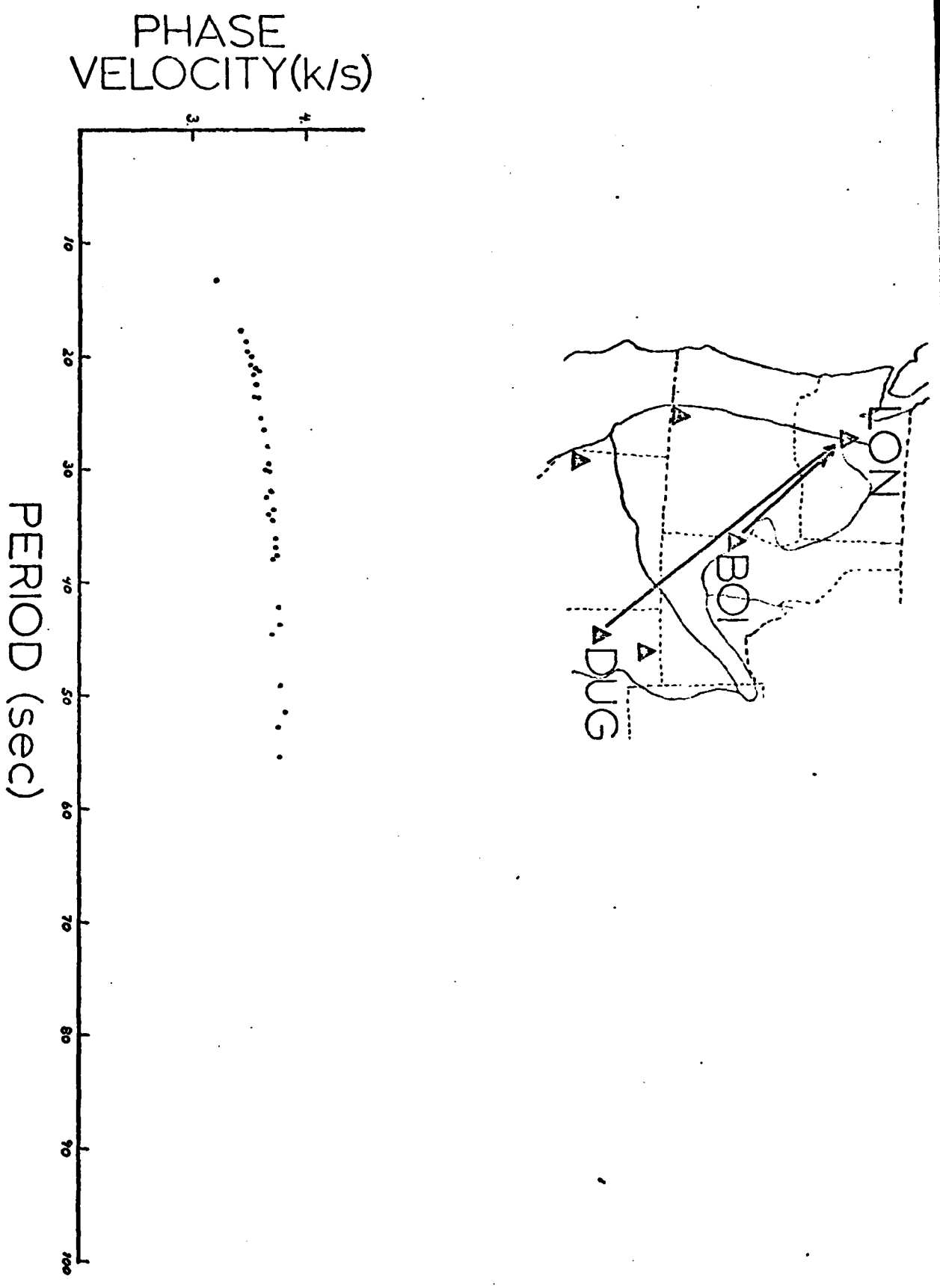
PHASE
VELOCITY(k/s)
3
4
10
20
30
40
50
60
70
80
90
100
PERIOD (sec)
ION
BOL
DUG

Figure 5

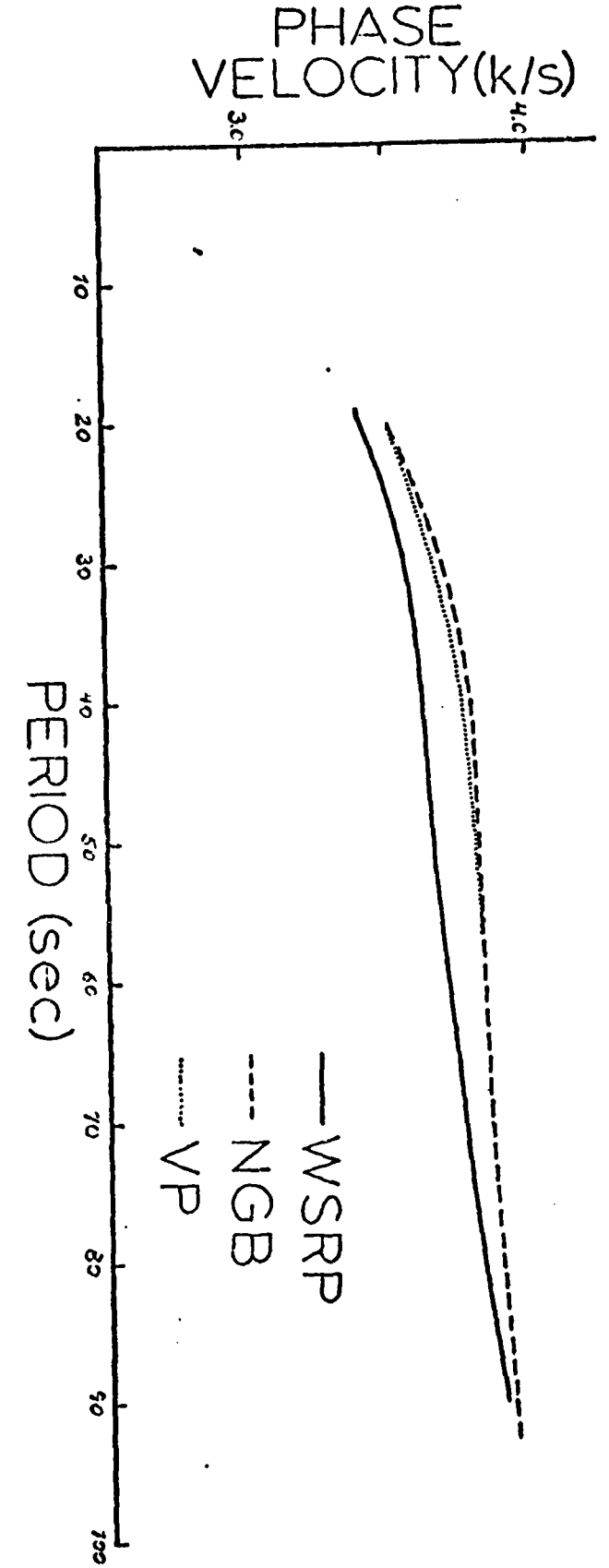
PHASE
VELOCITY(k/s)
3.0
4.0
10
20
30
40
50
60
70
80
90
100
PERIOD (sec)
—WSRP
---NGB
.....VP

Figure 6

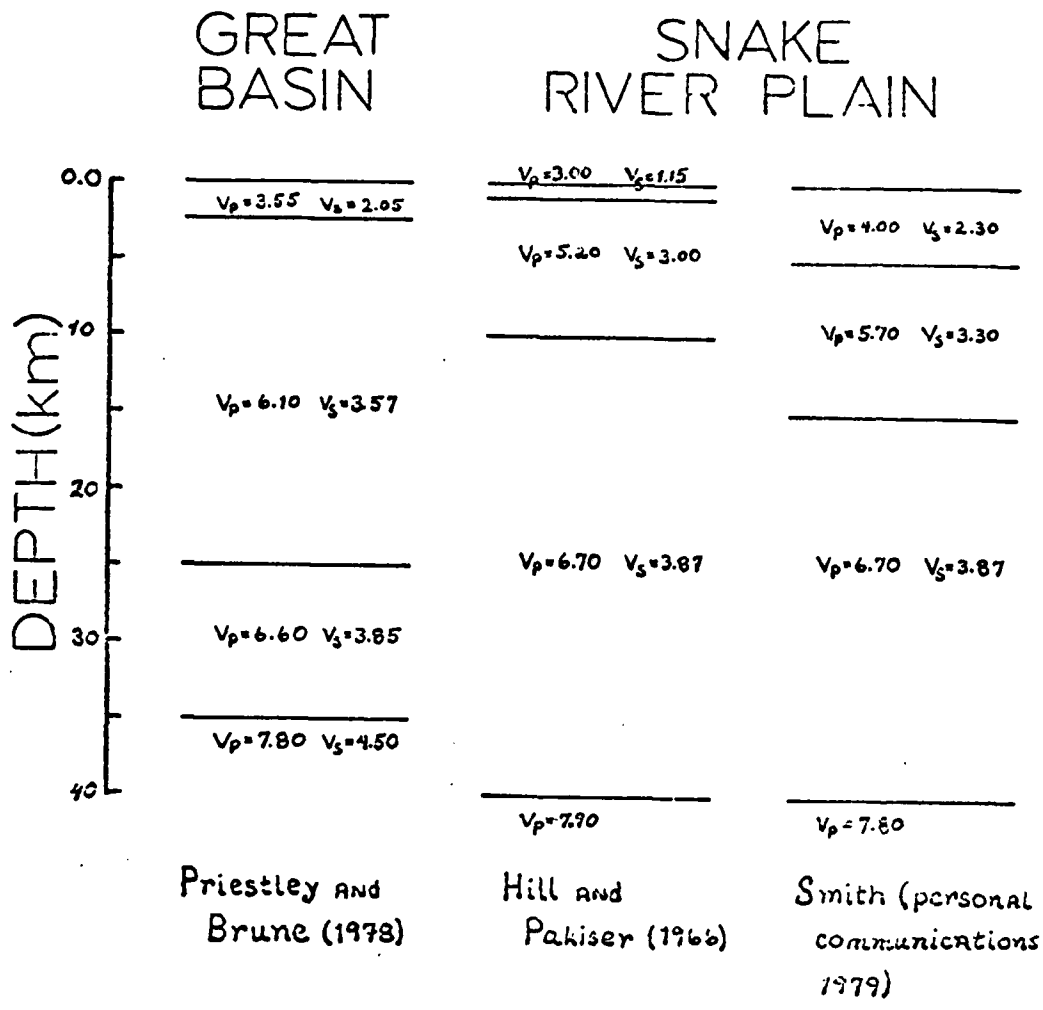
GREAT BASIN
SNAKE RIVER PLAIN
DEPTH (km)
0.0
10
20
30
40
Vp = 3.55 Vs = 2.05
Vp = 6.10 Vs = 3.57
Vp = 6.60 Vs = 3.85
Vp = 7.80 Vs = 4.50
Priestley AND Brune (1978)
Vp = 3.00 Vs = 1.15
Vp = 5.20 Vs = 3.00
Vp = 6.70 Vs = 3.87
Vp = 7.90
Hill AND Pakiser (1966)
Vp = 4.00 Vs = 2.30
Vp = 5.70 Vs = 3.30
Vp = 6.70 Vs = 3.87
Vp = 7.80
Smith (personal communications 1979)

Figure 7

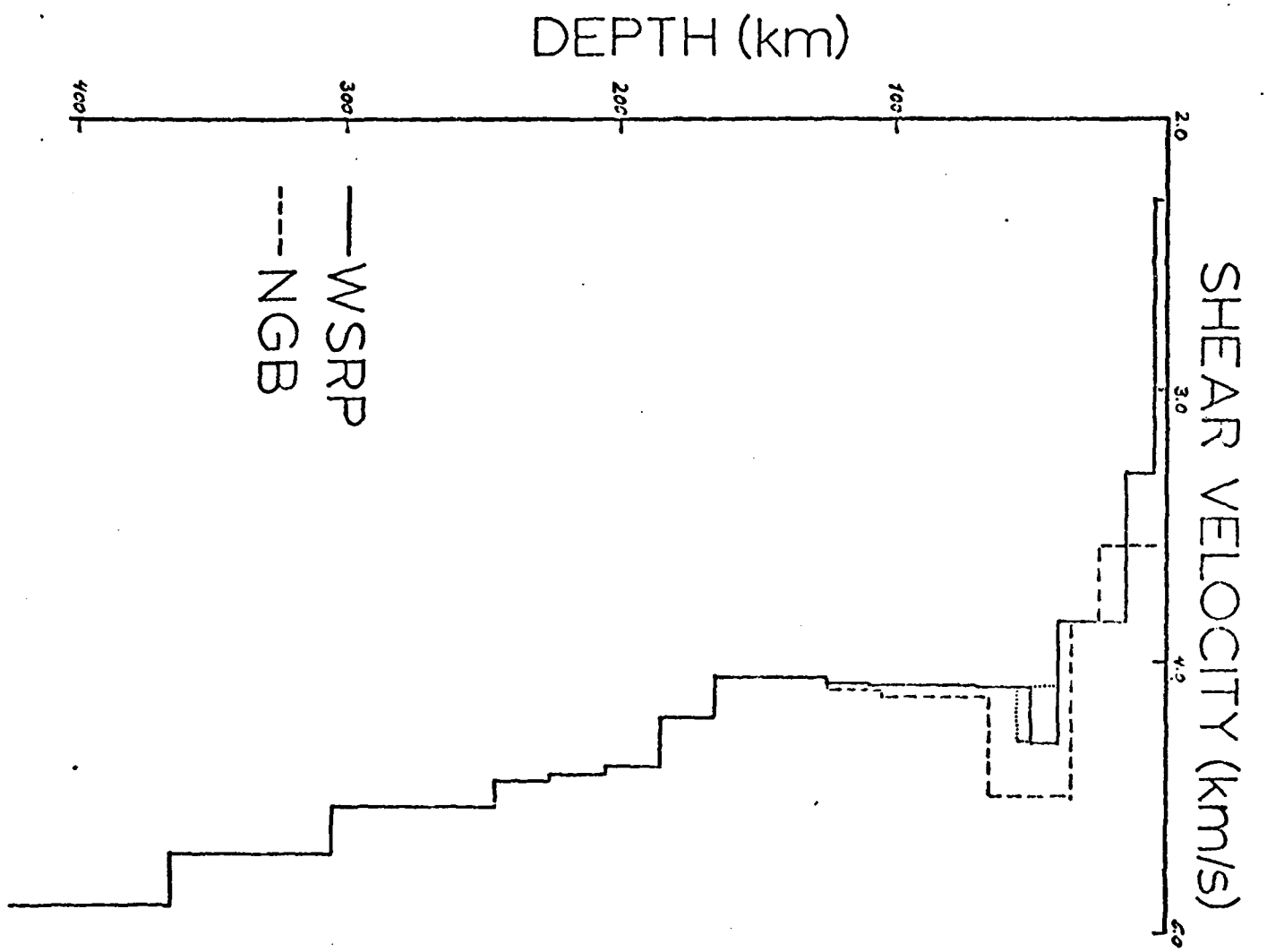
DEPTH (km)
400
300
200
100
2.0
3.0
4.9
6.0
SHEAR VELOCITY (km/s)
WSRP
NGB

Figure 8

APPENDIX A

Research Efforts: Great Basin

HIGHER MODE SURFACE WAVES AND STRUCTURE OF THE GREAT BASIN OF NEVADA AND WESTERN UTAH

Keith Priestley

Seismological Laboratory
Mackay School of Mines
University of Nevada
Reno, Nevada 89557

John A. Orcutt

Geological Research Division
Scripps Institution of Oceanography
University of California, San Diego
La Jolla, California 92093

James N. Brune

Institute of Geophysics and Planetary Physics
Scripps Institution of Oceanography
University of California, San Diego
La Jolla, California 92093

November 1979

ABSTRACT

Observed seismograms and dispersion data for crust and mantle higher mode surface waves in the Great Basin are compared with theoretical seismograms and dispersion curves computed for the GREAT BASIN model of Priestley and Brune (1978). This structure was originally derived from fundamental mode surface wave and refraction data. Phases identified as Sa [T ~ 13 sec] are observed to have a phase velocity of 4.50 ±0.03 km s^{-1}. Crustal 2nd Rayleigh mode (first shear mode) waves have predominant periods varying from about 5 seconds on some paths to about 8 seconds on others.

The observed excitation and phase velocity of the Sn phase are in agreement with theoretical seismograms and computed phase velocities for a modified GREAT BASIN model. The agreement provides added support, in an unexpected way, for the existence of a mantle lid of velocity about 4.5 km s^{-1} in the Great Basin.

The crustal higher model group velocity observations, i.e., the predominant periods of the 2nd Rayleigh mode along various paths, reflect variations in crustal thickness within the Great Basin. Crustal thicknesses of approximately 25 km are indicated for some paths in northwestern Nevada and southeastern Oregon whereas crustal thicknesses of greater than 35 km are indicated for east central Nevada. The crustal thickness of 35 km in the GREAT BASIN model is probably most appropriate for the central part of the Great Basin.

INTRODUCTION

In a previous paper (Priestley and Brune, 1978), fundamental mode surface wave dispersion was measured for a number of paths in the Great Basin of Nevada and western Utah. Using this data and existing refraction data, an average structural model was derived for the Great Basin. This model, referred to as the GREAT BASIN model, has a 3-layer crust of thickness 35 km, an upper mantle lid of shear velocity 4.5 km/sec and thickness 29 km, and an extreme low velocity layer of shear velocity about 4.1 km/sec and thickness about 120 km (Table 1). The pronounced low velocity zone in this model is similar to that found by Knopoff and Schlue (1972) for the East African Rift. This result supports the conclusion that the Great Basin is a zone of rifting.

Some of the questions that are suggested by the Priestley and Brune (1978) result are:

1. How much variation in crustal thickness occurs within the Great Basin? Some evidence for such variations, based on observed fundamental mode surface wave dispersion was discussed in their paper.
2. How certain is the existence and proposed 30-km thickness of the upper mantle lid of shear velocity 4.5 km/sec? This is an interesting question because of suggestions that in zones of rifting, the low velocity zone may extend to the crust and thus a lid over the low velocity zone, typically found in more stable areas, might not be present.

To help answer these questions we have searched for higher mode surface wave data which might provide independent evidence concerning the structure of the Great Basin. For certain aspects of earth structure higher mode data can often provide better resolution than fundamental mode data.

We present results for two types of higher mode data (Figure 1):

1. Sa propagating between the stations Reno and Tonopah from earthquakes off the coast of Oregon and Washington: Since this phase is travelling in the upper mantle its velocity might provide a constraint on the lid velocity.
2. 2nd Rayleigh mode (1st shear mode) surface waves propagating along a number of paths within the Great Basin: This mode has a steep group velocity curve near the period of crustal resonance. The period of this steep part of the curve is readily measured and is directly proportional to the crustal thickness (Oliver and Ewing, 1958) thus it can be used as a straightforward method of determining average crustal thickness over a given path and of observing variations in crustal thickness from path to path.

DATA

Sa: We have observed a very clear Sa phase at REN and TNP from earthquakes off the coast of Oregon and Washington at ranges between 1300 and 1700 km. Since the epicenters of the earthquakes used are nearly in line with the stations REN and TNP, we have been able to measure the phase velocity of its predominant period by phase correlation

between REN and TNP. Figure 2a shows examples of this phase. It has a predominant period of about 13 seconds (range from about 12-15 sec) and an arrival time about 20 sec later than the arrival time expected for Sn. Its group arrival time corresponds to a group velocity between roughly 4.0 and 4.5 km/sec. Because it consists of a group of relatively long period energy, its group velocity cannot be determined as accurately as its phase velocity. The phase velocity data, determined from correlations of peaks and troughs between REN and TNP, is summarized in Table 2. The estimated phase velocity at a period of 13 sec from 4 observations is 4.50 ±.03 km/sec. This result will be compared with theoretical computations in the next section.

2nd Rayleigh Mode: The second Rayleigh mode is commonly observed on long period vertical seismograms as a train of waves of relatively slowly varying period extending from near the expected S-wave arrival time to the arrival of the long period fundamental mode Rayleigh wave. Examples of second Rayleigh mode data used in this study are shown in Figure 2b. Because the period changes slowly with time (i.e., the dispersion is so great) it is often difficult to determine the slope of the group velocity very accurately. However, for the same reason, the period of the waves can be determined quite accurately. Theoretical calculations show that the predominant period of the steep portion of the group velocity curve is approximately proportional to average crustal thickness (Oliver and Ewing, 1958), and hence is very useful in determining average crustal thickness.

We have measured the predominant period of the crustal 2nd Rayleigh mode for a number of paths in the Great Basin. The results are presented

in Table 3. In some cases we were able to approximately estimate the slope of the dispersion curve (i.e., we could observe definite dispersions in the wave train) and in these cases we have indicated a range in velocities and periods.

COMPARISON WITH THEORETICAL CALCULATIONS

To interpret the data presented above, we have made two types of theoretical calculations for the GREAT BASIN model. First, we have computed theoretical seismograms using a direct Wavenumber Integration program developed by Apsel (1979) and the WKBJ method of Chapman (1978). Second, we have computed phase velocity, group velocity and particle motion diagrams using the normal mode program of Harkrider (1964, 1970).

Theoretical Seismograms: Using the Wavenumber Integration program we have calculated theoretical seismograms for the GREAT BASIN model over a range of distances to illustrate the character of the theoretical seismograms. In computing the theoretical seismcgrams we have assumed a double couple point source corrected for Q_β assuming a value of 500 in the lithosphere and 115 in the low velocity zone (Brune, 1977; Jordan and Sipkin, 1977) and corrected for instrument response for a Press-Ewing 15-90 long period seismograph. These results are presented in Figure 3. The overall character of theoretical seismograms are remarkably similar to the observations in Figure 2a indicating that the GREAT BASIN model corresponds closely to the earth structure of this region.

The period and phase velocity of the Sa phase can be determined directly from the theoretical seismograms using the same technique as for the experimental data. The predominant period and phase velocity

of the Sa phase on the theoretical seismograms is 13 seconds and 4.51 km/sec respectively, in excellent agreement with the period and phase velocity of the observed Sa phases.

Theoretical Dispersion Curves and Particle Motion Diagrams for Sa: Sa is typically observed as a pulse early in the surface wave train at large ranges from 60°- 110° (for example, Brune, 1965; Schwab et al., 1974; Kausel et al., 1977). Our observation of a sharp arrival near the beginning of the surface wave train with a phase velocity of 4.5 km s^{-1} and an apparent period of 12-15 seconds has led us to adopt the same nomenclature from 10°-16°. However, in this distance range we shall demonstrate that a ray theoretical approach for seismogram synthesis is the preferred method vis-a-vis the modal technique competitive at the larger ranges. Nevertheless, the concepts associated with modal synthesis provide insight into the behavior of this phase.

To identify and interpret the particular higher modes contributing to the observed data, we have computed higher mode phase velocity, group velocity and particle motion diagrams for the GREAT BASIN model using the normal mode computer program of Harkrider (1964, 1970) (Figures 4 through 6). The observed Sa phase consists of waves propagating with predominant periods of 12-15 sec and with a phase velocity, early in the wavetrain, of 4.5 km s^{-1}. This pulse may be thought of as the superposition of a number of higher modes covering a range of frequencies and propagating with phase velocities of 4.5 km s^{-1} and above. In fact, from the higher mode Rayleigh wave phase velocity curves (Figure 4) it can be seen that the observed phase is primarily composed of energy of the second and higher Rayleigh modes. The phase velocity curves illustrated are

reminiscent of the dispersion curves used by Kausel et al. (1977) in the treatment of oceanic Sa. Figure 5 is the energy density vs. depth plot for the third higher mode at 12.25 seconds period and phase velocity 4.54 km s^{-1}. Peaks in the energy distribution occur in the mantle lid, within the low velocity zone and in the 4.5 km s^{-1} layer at the base of the low velocity zone. For all the relevant modes, the "turning point" occurs at depths of approximately 200 km and greater (Kausel et al., 1977). "Turning point," of course, refers to the depth at which the vertical or radial wave functions for a mode of given frequency and phase velocity begin to decay in an exponential-like manner with increasing depth or decreasing radius.

Effect of Variation in Thickness of Mantle Lid: If we look upon the Sa phase as a sum of normal modes then we might expect, on the basis of particle motion diagrams such as shown in Figure 5, that varying the lid thickness might have a large effect on its character. On the other hand, if we regard it as a refracted wave travelling in the upper mantle we might expect the lid thickness to have little effect on its character since the wave turns at depths below the low velocity zone. Thus, although the shape of the particle motion (or energy density) versus depth curves might vary considerably as the lid thickness changes, the long period Sa pulse, composed of a superposition of several modes, will be constructed in such a way as to preserve the character of the long period Sa phase as essentially a pulse of refracted energy turning in the upper mantle.

Theoretical seismograms calculated by Brune and Dorman (1963) for their CANSD model clearly showed the long period Sa phase (predominant period about 12 sec, phase velocity about 4.6 km/s). On the other hand, their theoretical seismograms for the case when the low velocity zone

was removed did not show this predominant pulse and hence they interpreted the phase as a guided wave in the low velocity channel. However, in their study the excitation of the various modes for a realistic source was not computed, but the amplitudes were assumed constant as a function of frequency for all modes. Thus they pointed out that their results were somewhat artificial and hence they deferred a final interpretation of this phase.

In the present study the true excitation of each mode is computed using the Wavenumber Integration method. Figure 7 shows theoretical vertical component seismograms for Rayleigh waves at a distance of 17 degrees and an azimuth of 22.5° from the strike for a vertical strike-slip fault for depths of 0, 5, 10, 15 and 20 km. The relative prominence of the long period Sa phase increases as the depth of the source increases. Between depths of 0 and 10 km the phase is strongly affected by free surface interactions and can be regarded as a variation in the excitation of various higher modes. The theoretical seismograms for depths greater than 10 km, especially the one for a depth of 20 km, compare favorably with the observed seismogram. The agreement is much better than might have been expected since the actual travel path from Vancouver Island to Tonopah, and in particular the ray turning point, is mostly outside the Basin and Range Province.

In order to investigate the effect of thinning the mantle lid we computed theoretical seismograms for models in which the low velocity zone is extended to shallower depths thus decreasing the lid thickness. All other parameters in the model were fixed. Theoretical seismograms for a source depth of 15 km and lid thicknesses of 29 km (the original

thickness in the GREAT BASIN model), 15 km and 7 km are shown in Figure 8 at an epicentral distance of 18°. As can be seen, the character of the long period Sa pulse is not greatly changed by thinning of the lid. Although small differences in the details of the synthetic seismograms are apparent, the stability of the wavetrains in the face of substantial changes in the lid thickness is striking. Inspection of the fundamental mode data in this example, however, shows that thinning of the lid makes a large change in the phase of the fundamental mode on the seismograms. Thus the phase velocity of the longer period fundamental mode data provides a good constraint on the lid thickness, and of course is in agreement with a lid thickness of 29 km.

Figure 9 illustrates a profile of seismograms for a source depth of 15 km from 4° to 23°. The prominence of the Sa phase is a strong function of position along the profile and is mirrored by the variation in the amplitude of the P wave. From this point of view, modeling Sa as the shear body wave turning below the low velocity zone in the vicinity of the 400 km discontinuity appears promising.

Seismograms of two events off the Oregon coast recorded at Reno and Tonopah are plotted with a profile of synthetic seismograms in Figure 10. The synthetics were computed from a modified GREAT BASIN model illustrated in Figure 11. The compressional velocity model is essentially the T7 structure of Burdick and Helmberger (1978). The shear velocity model was constructed from the GREAT BASIN model except that the variation of velocity with depth is smoother and the upper mantle discontinuities are modeled after the T7 velocity structure assuming a Poisson's ratio of 0.25. The synthetic seismograms were computed with the WKBJ method (Chapman, 1978) and attenuation was modeled with a Futterman Q operator (Futterman, 1962)

assuming a T* of 3.0. The synthetics were convolved with a 15/90 Press-Ewing long period seismograph and a source function consisting of a double couple vertical strike-slip event buried 15 km. The rays used included S, sS and pS. The general character of the seismograms is well-modeled by the ray theory although we only seek to argue that the observations are consistent with the modified Great Basin or T7 structures. The individual observations have been shifted, at most, a few seconds in time to provide alignment with the synthetics. The secondary arrivals clearly seen in the observations at less than 14 degrees are associated with the "reflection" from the 400 km discontinuity (marked 400 in Figure 10). The initial arrivals result from a caustic formed by the increasing velocity below the low velocity zone. It is important to note that the travel time curve for the first rays to turn below the low velocity zone is retrograde. Near the caustic this branch generates substantial amplitudes with a phase velocity near the lithosphere lid velocity of 4.5 km s^{-1}. As the range increases beyond 14 degrees the pulse becomes considerably more simple and the phase velocity increases.

The model used to compute the synthetic seismograms in Figures 3, 7, 8 and 9 was a coarse 12-layer analog of the original GREAT BASIN model. Although the surface waves are accurately represented, the body waves are quite complex because of the reverberations within layers and reflections from the large discontinuities which result from the discreteness of the model. Green's functions for the vertical components at 12° and 14° are illustrated in Figure 12. The source was a vertical strike-slip event buried at a depth of 15 km and the displacement scale applies to both sets of synthetics for a source moment of 10^{25} dyne-cm. Although the amplitude of the displacements are nearly the same, the Wavenumber Integration (WI)

synthetics are much more complex. Because of the expense of the Wavenumber Integration technique and its unfavorable dependence on the number of layers, we were unable to adequately represent the earth structure to produce realistic body waves. The WKBJ synthetics, on the other hand, can be economically exploited to synthesize the ground motion for this particular problem.

In a laterally homogeneous earth model the observation of the Sa phase at a velocity of 4.5 km s^{-1} implies that the lithosphere lid has a velocity of approximately 4.5 km s^{-1}. However, in this case the rays which formed the seismograms turned under the Cascade ranges of the northwestern United States and the implications are not as strong since the mantle structure under the Cascades and in the Great Basin may well be different. We may only assert that, given our interpretation of the Sa phase and flat, homogeneous layers under the receivers, the lid velocity in the Great Basin does not exceed 4.5 km s^{-1}. The actual velocity could, in fact, be slightly less. Table 4 details the modified GREAT BASIN structure.

Theoretical Dispersion Curves for Higher Rayleigh Modes and Variations in Crustal Thickness: Figure 6 gives the higher Rayleigh mode group velocity curves computed for the GREAT BASIN model. The GREAT BASIN model has a 35-km thick crust and the predominant period of the crustal second Rayleigh mode is 7 to 8 seconds. The observed data for the crustal second Rayleigh mode is indicated by the short, heavy line segments. As mentioned above, the predominant period of the steep portion of the group velocity curve is approximately proportional to the average crustal thickness along the path of propagation. We may approximately determine the average crustal thickness for the observed paths by directly comparing

the observed and theoretical predominant period of the crustal second Rayleigh mode. Thus we obtain the estimated crustal thickness listed in the third column of Table 3 and shown in Figure 13.

The observed variations in predominant period of the crustal higher mode and the inferred variations in crustal thickness may be correlated with the fraction of the travel path within the Battle Mountain heat flow high. Five of the paths for which crustal higher modes were observed cross this zone, an area of high continental heat flow trending northeastward from the vicinity of Reno across the northern Great Basin (Sass et al., 1976). The predominant period for the Idaho-Reno path corresponds to a crustal thickness of 37 km. This path crosses the Battle Mountain high but includes a large section of path in the Snake River Plain and Oregon Volcanic Province. The Adel-Dugway and Adel-Tonopah paths (29.5 km and 31 km average crustal thickness, respectively) cross the Battle Mountain high but include portions of the volcanic province and areas of more normal Great Basin heat flow. The two remaining paths in the northern Great Basin, Adel-Reno and Winnemucca-Dugway (both 25 km average crustal thickness), are nearly confined to the region of high heat flow. Thus crustal thinning within the Battle Mountain heat flow high is indicated by the higher mode data. This result is supported by travel-time data from Nevada Test Site explosions through the same area (Stauber and Boore, 1978; Priestley and Fezie, 1979).

The fundamental mode data of Priestley and Brune (1978) was confined to the central Great Basin. The three remaining paths for which crustal higher modes were observed (S.W. Utah-Reno, S.W. Utah-Tonopah, Bishop, GA-Logan) indicate a crustal thickness near 35 km. These paths through the central Great Basin agree with the crustal model of the GREAT BASIN model.

SUMMARY

1. Higher mode surface wave observations within the Great Basin of Nevada and western Utah have been presented. These consist of an Sa phase observed for a number of earthquakes located off the coast of Oregon and Washington, and crustal higher modes for moderate earthquakes located within the Great Basin.

2. The 4.50 ±0.03 k/s phase velocity of the Sa phase is in excellent agreement with synthetic seismograms computed for the modified GREAT BASIN structure. The observed phase velocity implies an upper bound on the shear velocity of the lithosphere lid but provides no constraint on the lid thickness. The phase velocity of fundamental mode Rayleigh waves remains the most important constraint on the lid thickness of about 29 km.

3. The crustal higher mode data indicates there are significant variations in the crustal thickness within the Great Basin. The fundamental mode data indicates an average crustal thickness of about 35 km for the whole Great Basin, however, across the northern Great Basin (the area of the Battle Mountain heat flow high), the higher mode Rayleigh wave data indicate that the crust thins to about 25-km thickness.

ACKNOWLEDGEMENTS

This research has been supported in part by the National Science Foundation under grant No. EAR79-22886 and by the Advanced Research Projects Agency and was monitored by the Air Force Office of Scientific Research under contracts F49620-77-C-0070 and F49620-79-C-0019.

REFERENCES

Apsel, R. J., Dynamic Green's functions for layered media and applications to boundary-value problems, Ph.D. thesis, University of California, San Diego, 1979.

Brune, J. and J. Dorman, Seismic waves and earth structure in the Canadian shield, Bull. Seismol. Soc. Amer., 53, 167-210, 1963.

Brune, J., the Sa phase from the Hindu Kush Earthquake of July 6, 1962, Pure Appl. Geophys., 62, p. 81, 1965.

Brune, J. N., Q of shear waves estimated from S-SS spectral ratios, Geophys. Res. Lett., 4, 179-181, 1977.

Burdick, L. J. and D. V. Helmberger, The upper mantle P velocity structure of the western United States, J. Geophys. Res., 83, 1699-1712, 1978.

Chapman, C. H., A new method for computing synthetic seismograms, Geophys. J. R. Astrol. Soc., 54, 481-518, 1978.

Futterman, W. I., Dispersive body waves, J. Geophys. Res., 67, 5279-5291, 1962.

Harkrider, D. G., Surface waves in multilayered elastic media. Part I. Rayleigh and Love Waves from buried sources in a multilayered elastic half-space, Bull. Seismol. Soc. Amer., 54, p. 627, 1964.

Harkrider, D. G., Surface waves in multilayered elastic media. Part II. Higher mode spectra and spectral ratios from point sources in plain layered earth models, Bull. Seismol. Soc. Amer., 60, p. 1937, 1970.

Jordan, T. H. and S. A. Sipkin, Estimation of the attenuation operator for multiple ScS waves, Geophys. Res. Lett., 4, 167-170, 1977.

Kausel, E. G., F. Schwab and E. Mantovani, Oceanic Sa, Geophys. J. R. astrol. Soc., 36, 737-742, 1974.

Knopoff, L. and J. Schlue, Rayleigh wave phase velocities for the path Addis Ababa-Nairobi, Tectonophysics, 15, p. 157, 1972.

Oliver, J. and M. Ewing, Normal modes of continental surface waves, Bull. Seismol. Soc. Amer., 48, 33, 1958.

Priestley, K. and J. Brune, Surface waves and the structure of the Great Basin of Nevada and Western Utah, Jour. Geophys. Res., 83, 2265, 1978.

Priestley, K. and G. Fezie, Crustal structure from Tonopah, Nevada to Bend, Oregon from seismic refraction measurements, to be submitted to Bull. Seismol. Soc. Amer.

Sass, J. H., W. H. Diment, A. H. Lackenbruch, B. V. Marshall, R. J. Munroe, T. H. Morse, Jr. and T. C. Urban, A new heat flow contour map of the conterminous United States, U.S. Geol. Survey Open-File Rept. 76, p. 756, 1976.

Schwab, F., E. Kausel and L. Knopoff, Interpretation of Sa for a shield structure, Geophys. J. R. astr. Soc., 36, 737-742, 1974.

TABLE 1. Great Basin Model

Layer Thickness H, km	Compressional Wave Velocity α, km/s	Shear Wave Velocity β, km/s	Density ρ, g/cm^3
2.5	3.55	2.05	2.20
22.5	6.10	3.57	2.82
10.0	6.60	3.85	2.84
29.0	7.80	4.50	3.30
40.0	7.80	4.12	3.30
16.0	7.81	4.10	3.40
20.0	7.85	4.05	3.40
20.0	7.87	4.05	3.42
20.0	7.92	4.06	3.44
20.0	8.00	4.38	3.46
20.0	8.10	4.41	3.48
20.0	8.20	4.44	3.49
60.0	8.35	4.53	3.53
60.0	8.66	4.70	3.58
60.0	8.96	4.90	3.63
60.0	9.29	5.13	3.75
60.0	9.65	5.34	3.91
60.0	9.97	5.53	4.05
100.0	10.31	5.76	4.21
100.0	10.71	6.03	4.40
100.0	11.10	6.23	4.56
	11.35	6.31	4.63

TABLE 2

EVENT	COMPONENT	AVERAGE PERIOD (sec)	PHASE VELOCITY (K/S)
October 16, 1967 1327:35.6 49.3°N 129.1°W	Z	12	4.47
	E	13	4.50
	N	13	4.50
February 7, 1968 0758:03.5 50.0°N 129.8°W	Z	12	4.50
	E	13	4.47
	N	13.5	4.60
February 6, 1968 0835:29.6 43.6°N 127.3°W	Z	13	4.51
	N	13	4.45

TABLE 3. Crustal Higher Modes

Event	Path	Period	Equivalent Crustal Thickness
10/41/67	S.W. Utah-Ren	7.0 sec	35 km
1/30/68	Winn.-Dug	5.0 sec	25 km
5/29/68	Adel -Dug	6.8 sec	34 km
	Adel -TNP	6.7 sec	33.5 km
	Adel -Ren	5.0 sec	25 km
6/ 4/68	Adel -Dug	6.7 sec	33.5 km
	Adel -TNP	6.7 sec	33.5 km
	Adel -Ren	5.0 sec	25 km
6/ 5/68	Adel -Dug	6.7 sec	33.5 km
	Adel -Ren	5.0 sec	25 km
4/26/69	Boise-Ren	8.5-6.5 sec	37 km
10/ 4/78	Bishop-Log	7.0 sec	35 km

TABLE 4. Modified GREAT BASIN Model

Depth (km)	Shear Velocity (km/s)	Depth (km)	Shear Velocity (km/s)	Depth (km)	Shear Velocity (km/s)
0.0	3.57	310.0	4.70	540.0	5.50
20.0	3.57	320.0	4.73	550.0	5.53
20.0	3.85	330.0	4.77	560.0	5.57
35.0	3.85	340.0	4.80	570.0	5.61
35.0	4.5	350.0	4.83	580.0	5.64
65.0	4.5	360.0	4.87	590.0	5.68
73.1	4.12	370.0	4.90	600.0	5.72
103.3	4.12	380.0	4.90	610.0	5.77
117.5	4.10	386.0	4.91	620.0	5.82
127.0	4.05	393.5	4.91	630.0	5.85
162.3	4.05	393.6	5.10	640.0	5.88
168.2	4.06	400.0	5.12	650.0	5.92
180.0	4.06	410.0	5.14	660.0	5.96
190.0	4.38	420.0	5.17	667.0	6.0
200.0	4.38	430.0	5.19	667.1	6.24
210.0	4.41	440.0	5.22	675.0	6.24
220.0	4.41	450.0	5.24	685.0	6.26
230.0	4.44	460.0	5.27	695.0	6.28
240.0	4.44	470.0	5.29		
250.0	4.53	480.0	5.32		
260.0	4.56	490.0	5.34		
270.0	4.59	500.0	5.37		
280.0	4.61	510.0	5.40		
290.0	4.64	520.0	5.43		
300.0	4.67	530.0	5.47		

Figure 1. Location map showing events analyzed and area studied; insert shows the relationship of the paths for which data was analyzed.

Figure 2a. Seismograms recorded at Reno and Tonopah for an earthquake off Vancouver Island. The Sa phase is shown as a pulse preceding the fundamental mode Rayleigh wave arrival.

Figure 2b. Seismograms for regional Great Basin earthquakes. For the Adel, Oregon earthquake seismogram recorded at Dugway, Utah, the higher mode data analyzed are the relatively monochromatic wave train preceding the fundamental mode Rayleigh wave. For the central Idaho earthquake seismogram recorded at Reno, Nevada, the crustal higher mode analyzed is the earlier arriving dispersed wave train.

Figure 3. Synthetic seismograms at ranges of 12° and 14° computed the Wavenumber Integration program. The source is buried at 15 km and consists of a vertical strike-slip double couple. The source time function is a triangle four seconds in duration and the resulting seismogram has been convolved with a Press-Ewing 15/90 instrument response. The "Sa" phase can be particularly clearly seen at a range of 14°.

Figure 4. Rayleigh wave dispersion curves for the GREAT BASIN model. The observed Sa phase corresponds to energy propagating primarily as second and higher Rayleigh modes.

Figure 5. Energy density diagram for the third higher Rayleigh mode at $T = 12.25$ sec and $C = 4.54$ km s^{-1}. The upper lobe is confined primarily to the mantle lid.

Figure 6. Rayleigh wave group velocity curves for the GREAT BASIN model. The group velocities observed for the crustal higher mode data are indicated by short line segments.

Figure 7. The effect of source depth upon seismograms computed for the GREAT BASIN model. The source is a vertical strike-slip event and the source time function is a triangle four seconds in duration. The seismograms have not been convolved with an instrument response and have been plotted on the same absolute scale.

Figure 8. The effect of lithosphere lid thickness upon seismograms computed for the GREAT BASIN model. The lithosphere lid has been thinned by increasing the thickness of the low velocity zone.

Figure 9. A profile of synthetic seismograms from 4° to 23°. The source depth is again 15 km and the pure Green's functions are illustrated.

Figure 10. Synthetic seismograms computed for the modified GREAT BASIN model compared to a sample suite of observations from the stations at Reno and Tonopah. The synthetics were computed with the WKBJ algorithm and convolved with a Press-Ewing 15/90 seismograph response. The branches labeled "LVZ" and "400 km discontinuity" refer to "reflected" branches from the increasing velocities below the low velocity zone and 400 km "discontinuity" respectively.

Figure 11. The modified GREAT BASIN model used in computing the synthetic seismograms in Figure 10.

Figure 12. A comparison of Wavenumber Integration (WI) and WKBJ seismograms computed at ranges of 12° and 14°. The Green's functions are illustrated and the same absolute scaling has been used in all four seismograms. WI synthetics were computed from the coarse GREAT BASIN model while the WKBJ seismograms were computed with the smooth modified GREAT BASIN structure.

Figure 13. Summary of 2nd Rayleigh mode dispersion results for average crustal thickness along various paths in the Great Basin.

Fig 1

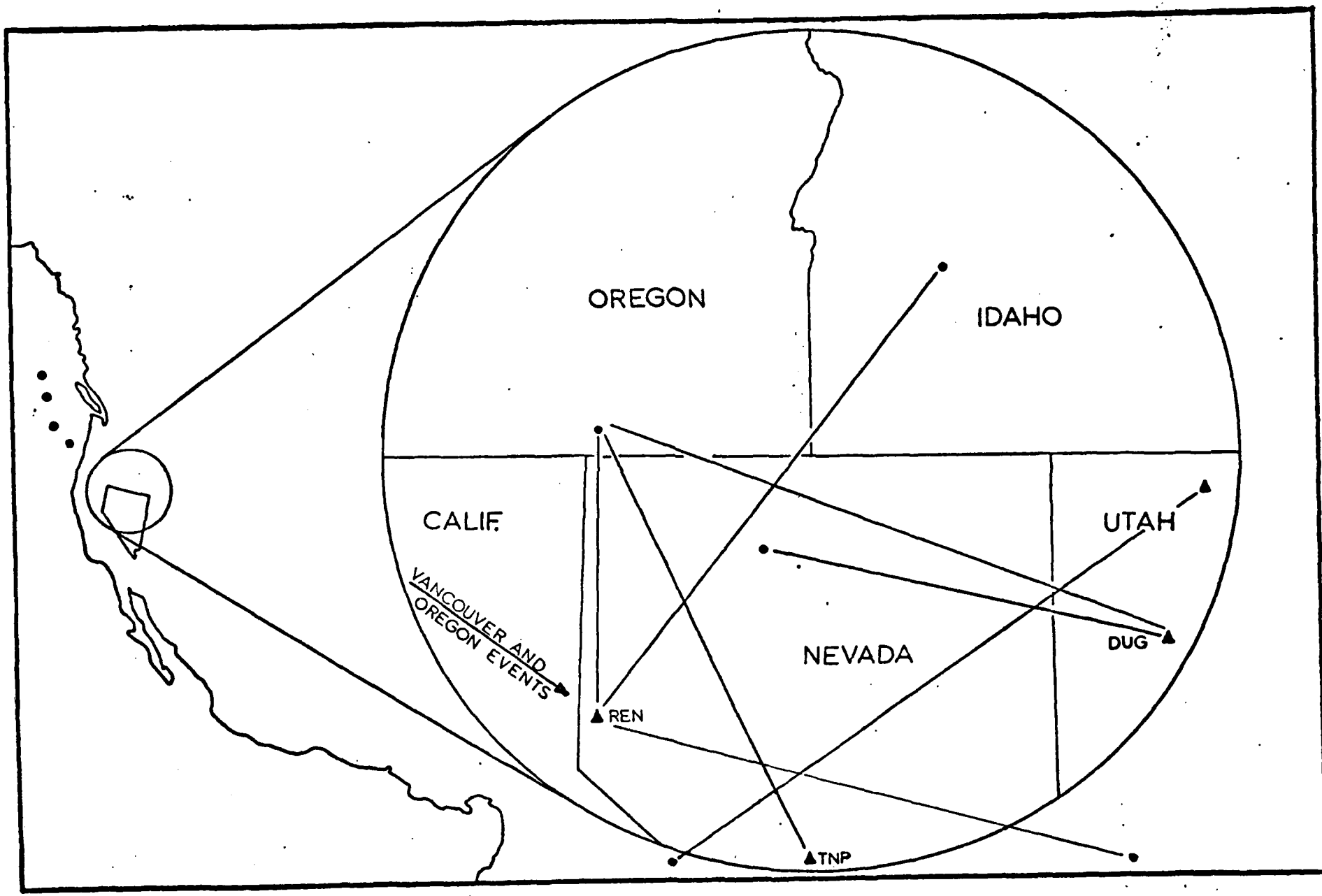
OREGON
IDAHO
CALIF.
UTAH
NEVADA
VANCOUVER AND OREGON EVENTS
REN
DUG
TNP

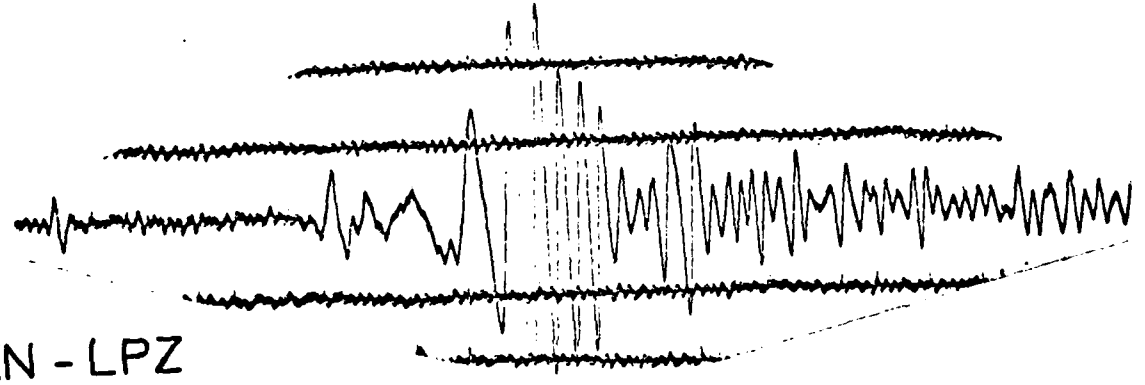

REN - LPZ

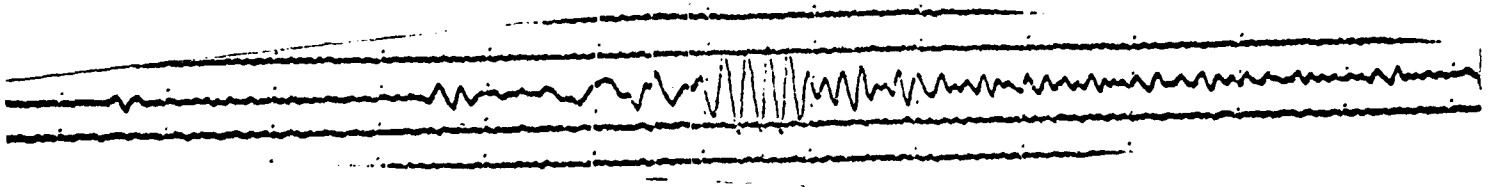

TNP - LPZ

VANCOUVER ISLAND REGION

FEB 1,1968 07 58 03.5 GMT 50.0° N 129.8° W

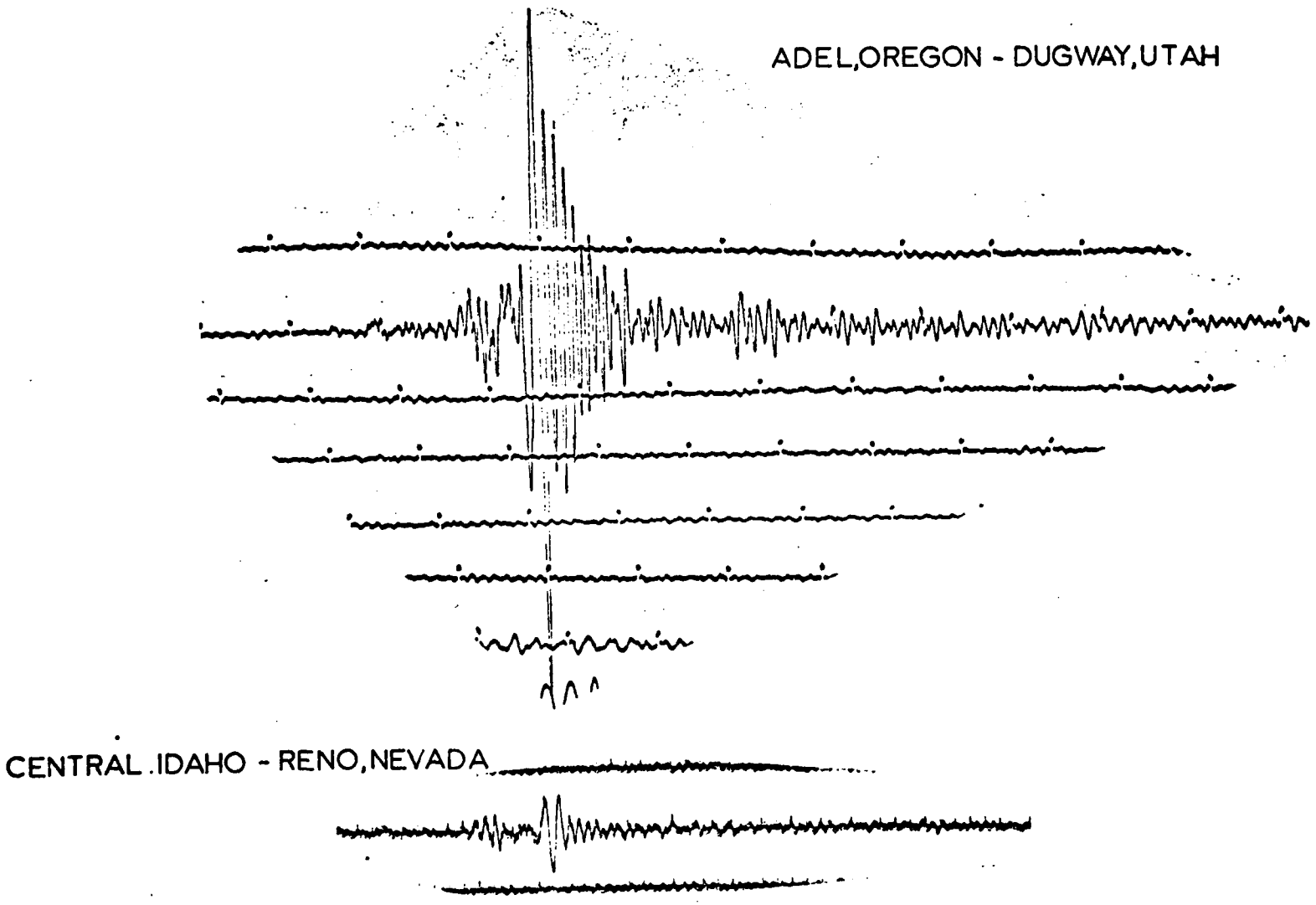
ADEL,OREGON - DUGWAY,UTAH
CENTRAL IDAHO - RENO,NEVADA

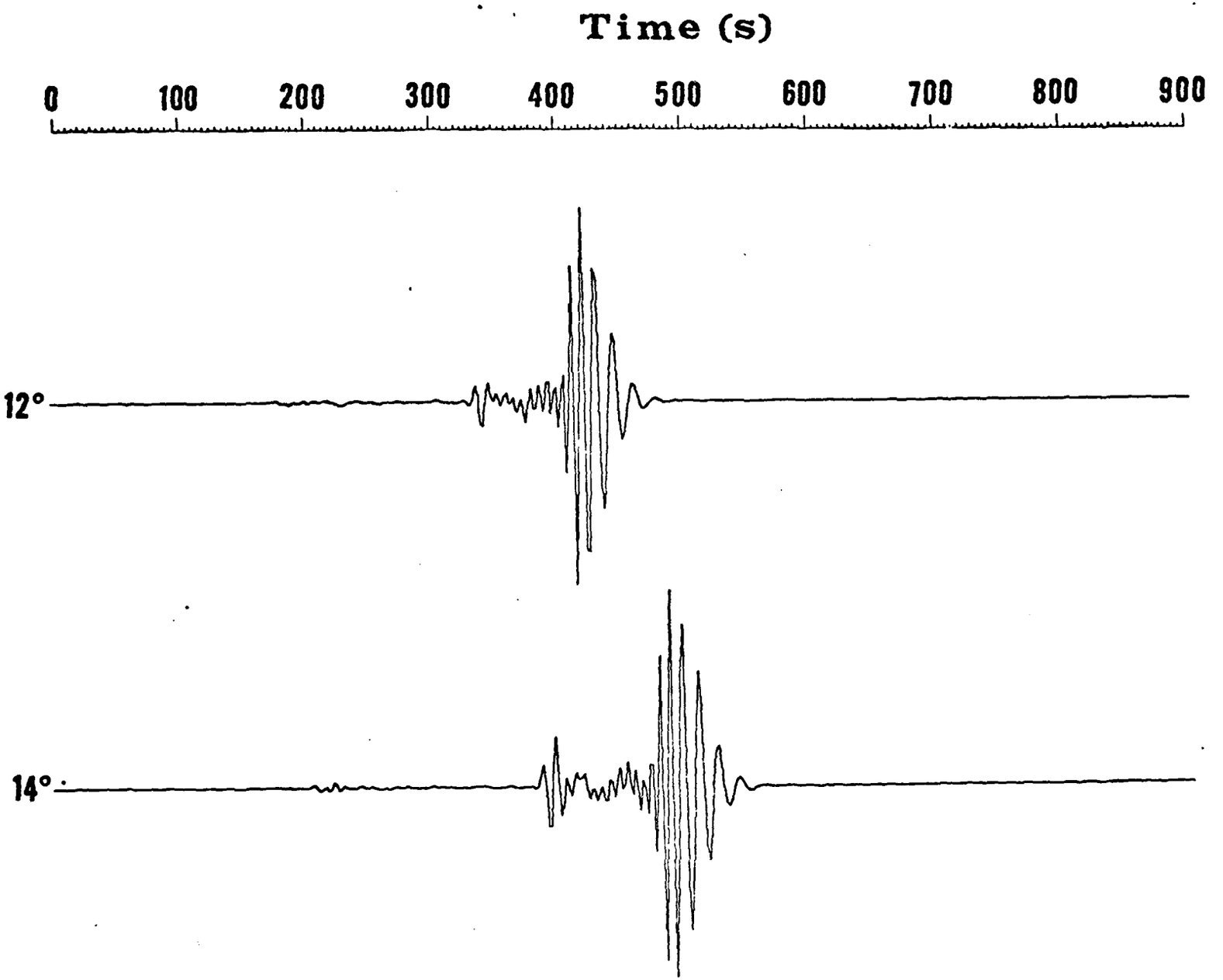
Time (s)
0
100
200
300
400
500
600
700
800
900
12°
14°

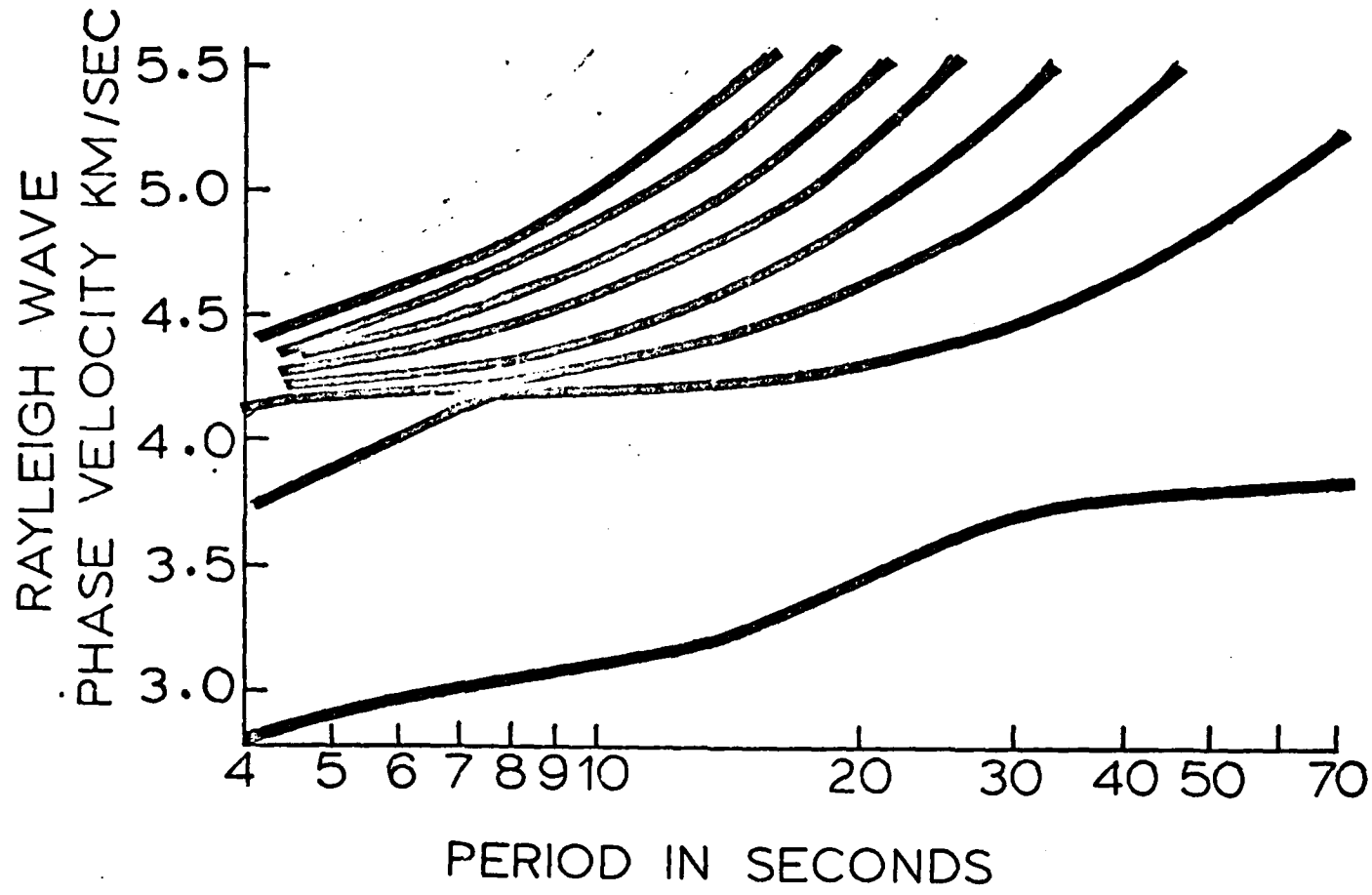
RAYLEIGH WAVE
PHASE VELOCITY KM/SEC
5.5
5.0
4.5
4.0
3.5
3.0
4 5 6 7 8 9 10 20 30 40 50 70
PERIOD IN SECONDS

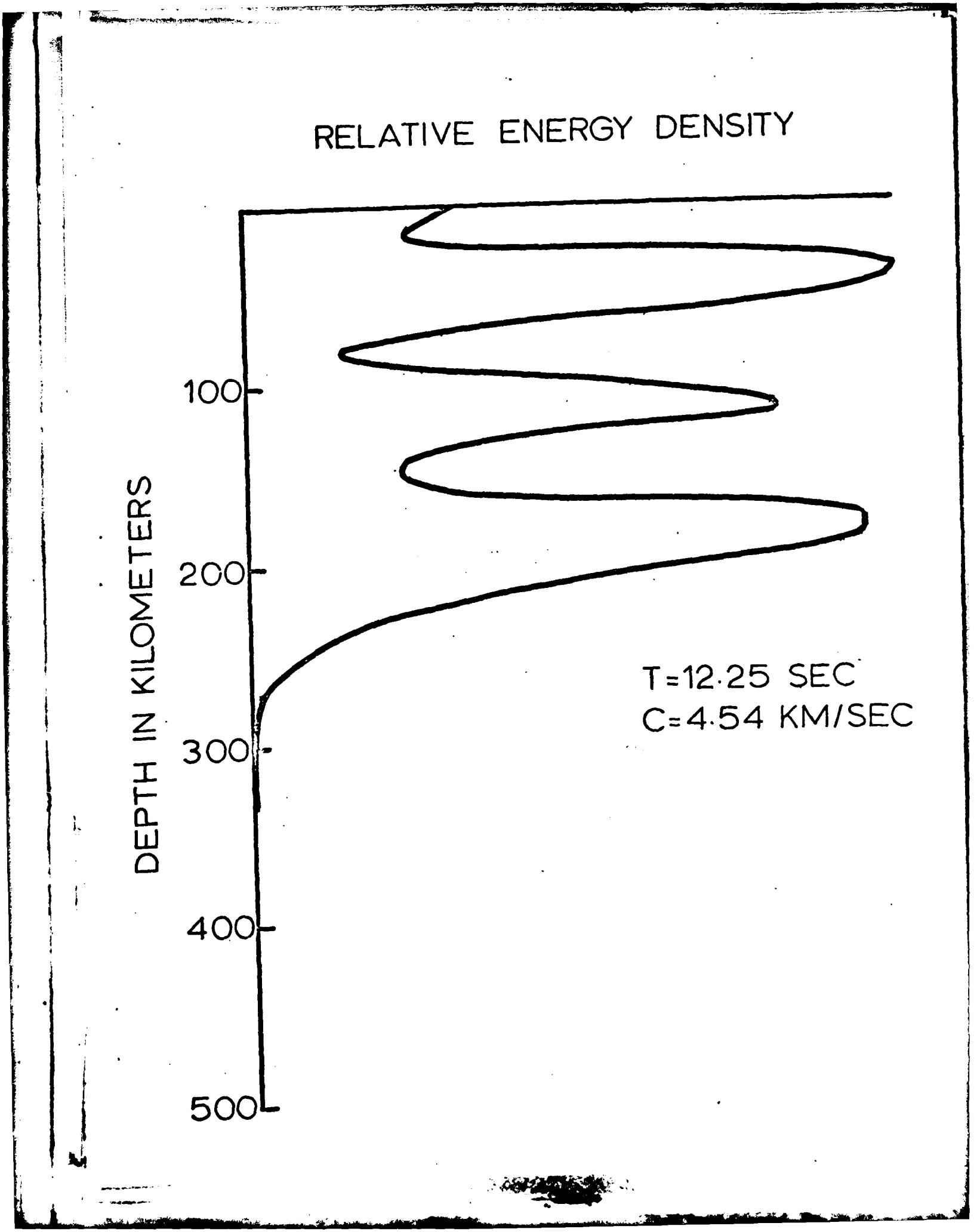
RELATIVE ENERGY DENSITY
DEPTH IN KILOMETERS
100
200
300
400
500
T=12.25 SEC
C=4.54 KM/SEC

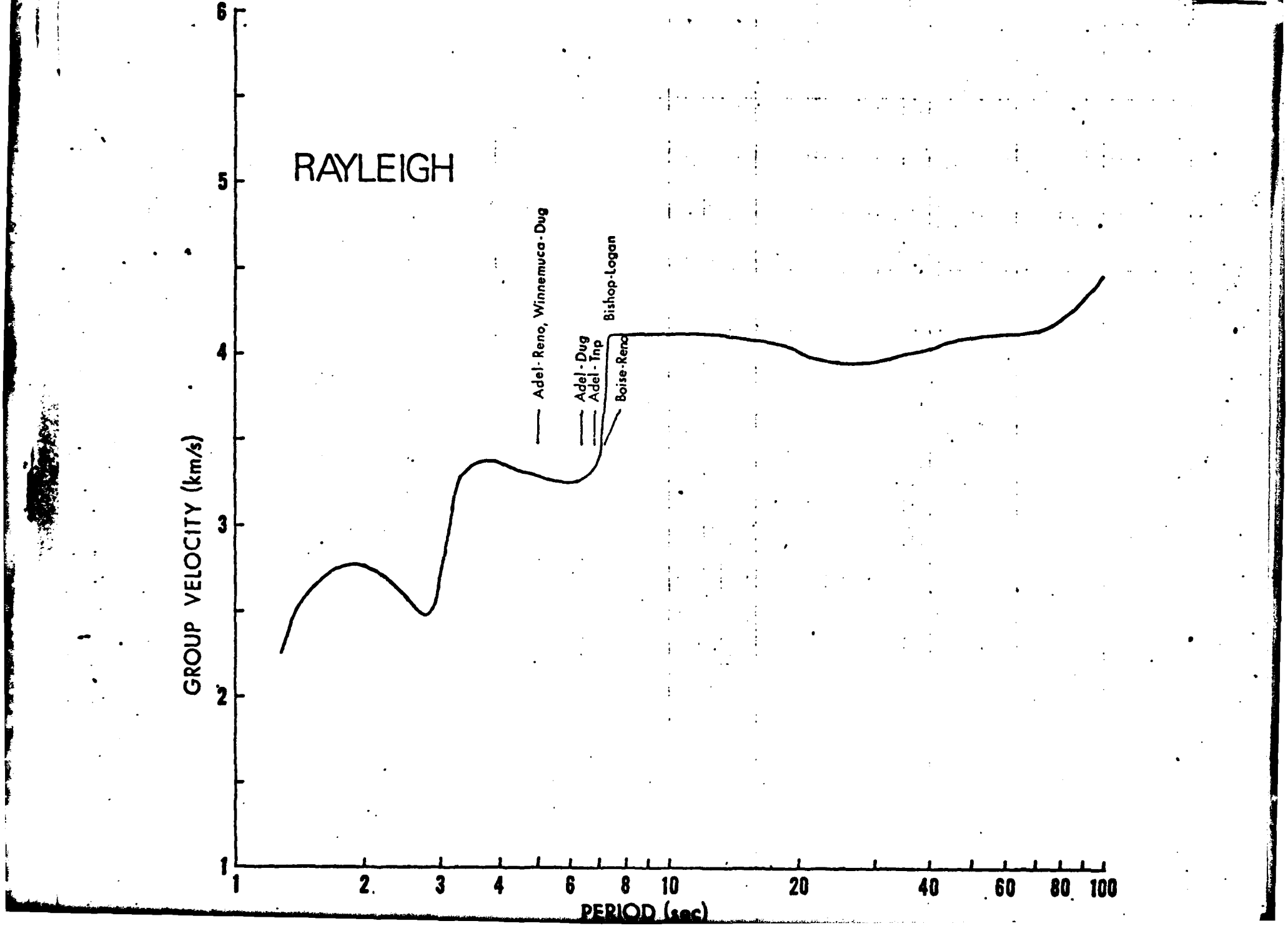
RAYLEIGH
GROUP VELOCITY (km/s)
PERIOD (sec)
Adel - Reno, Winnemuca - Dug
Adel - Dug
Adel - Tnp
Bishop - Logan
Boise - Reno
1
2
3
4
5
6
1
2.
3
4
6
8
10
20
40
60
80
100

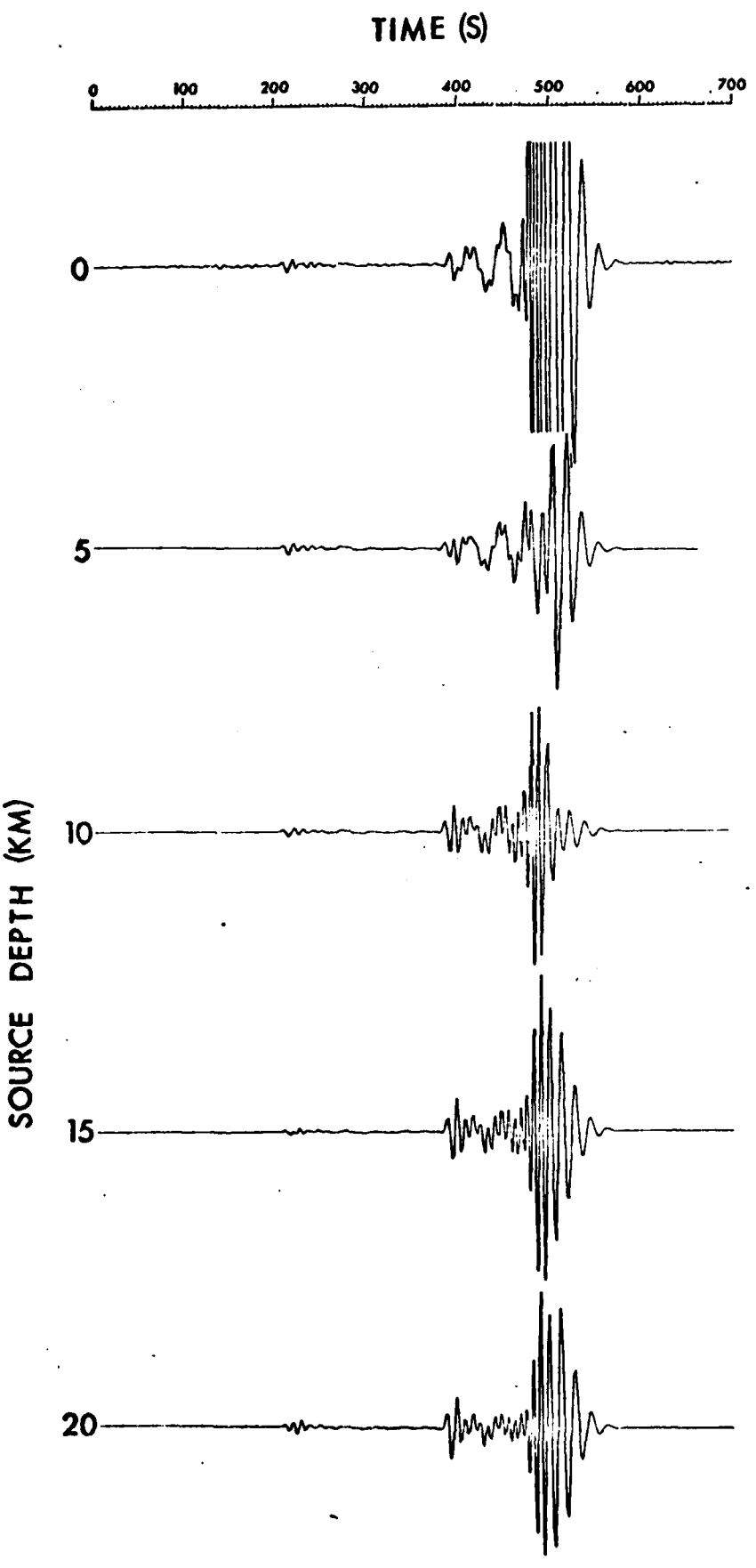
TIME (S)
0
100
200
300
400
500
600
700
SOURCE DEPTH (KM)
0
5
10
15
20

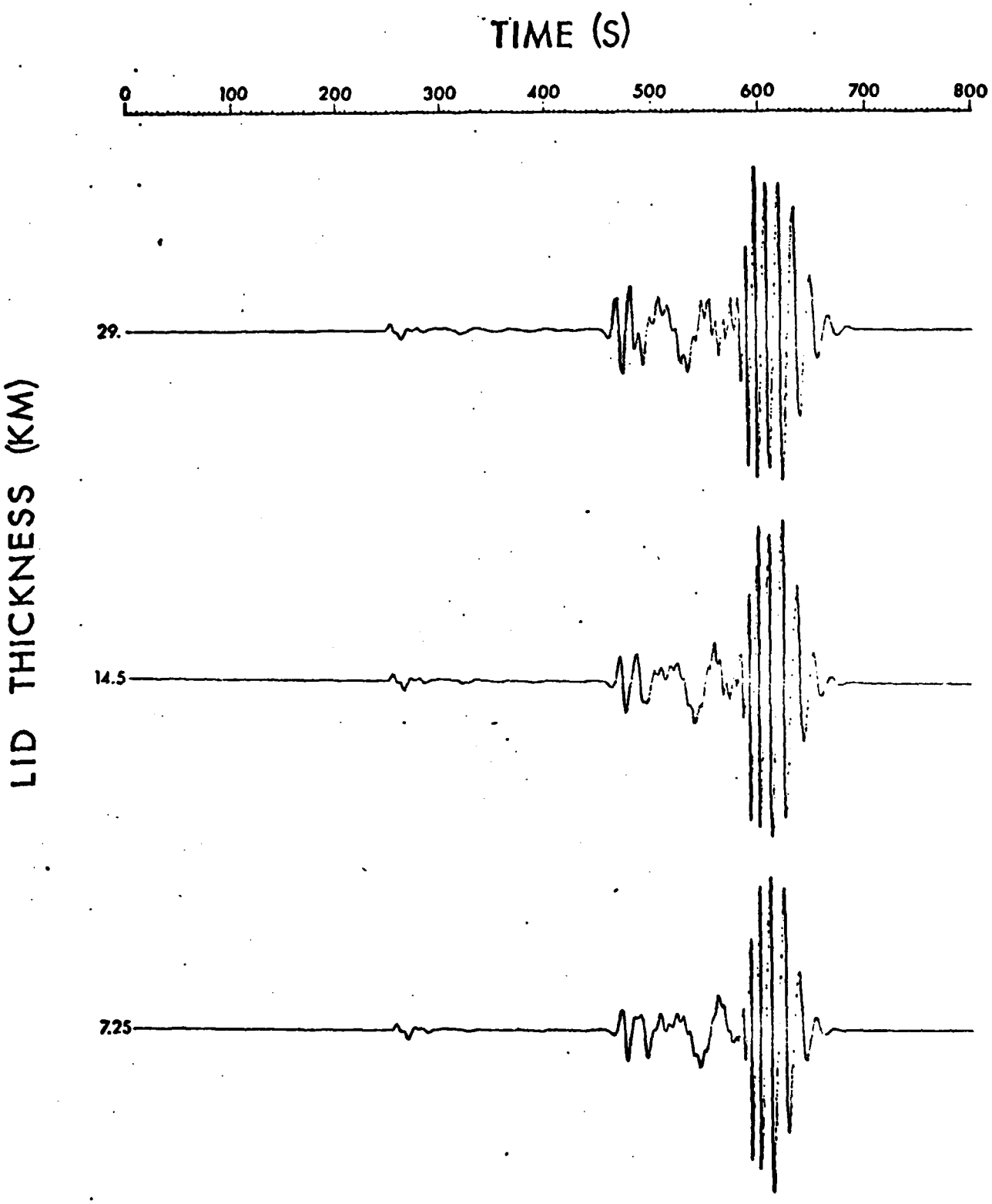
TIME (S)
0
100
200
300
400
500
600
700
800
LID THICKNESS (KM)
29.
14.5
7.25

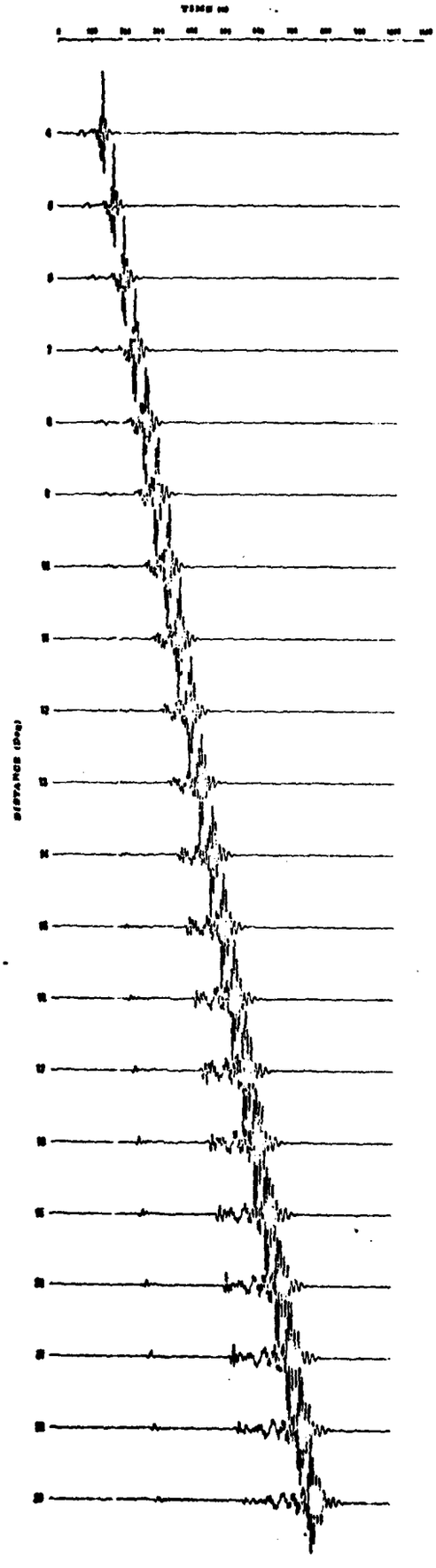

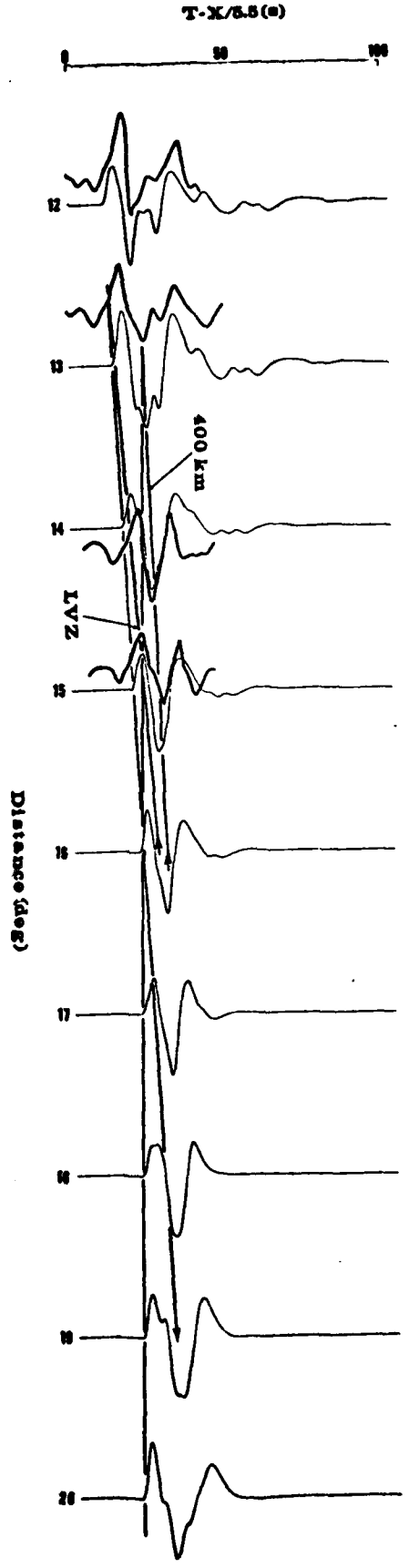
T-X/5.5(s)
0
50
100
12
13
400 km
14
LVZ
15
16
17
18
19
20
Distance (deg)

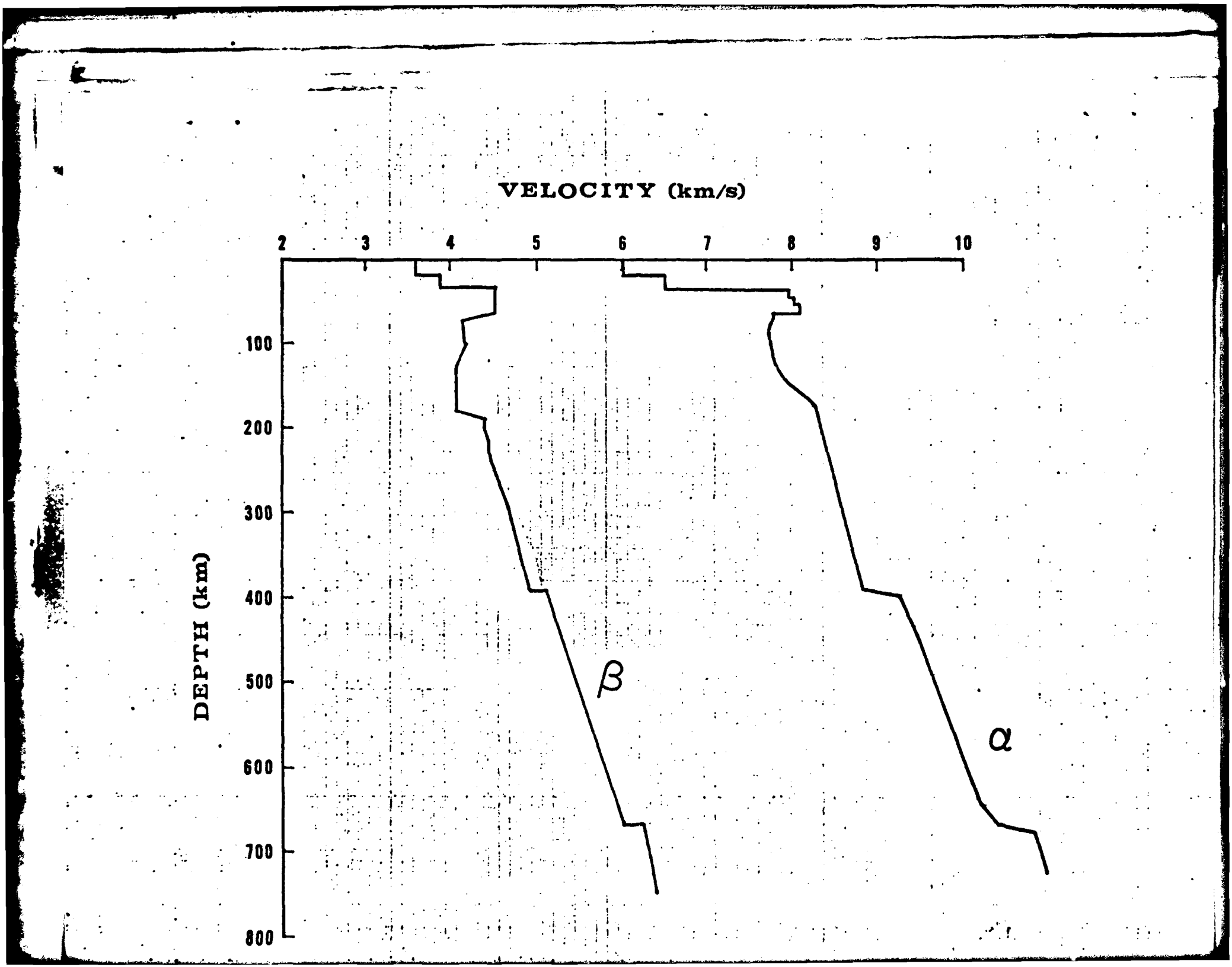
VELOCITY (km/s)
2
3
4
5
6
7
8
9
10
DEPTH (km)
100
200
300
400
500
600
700
800
β
α

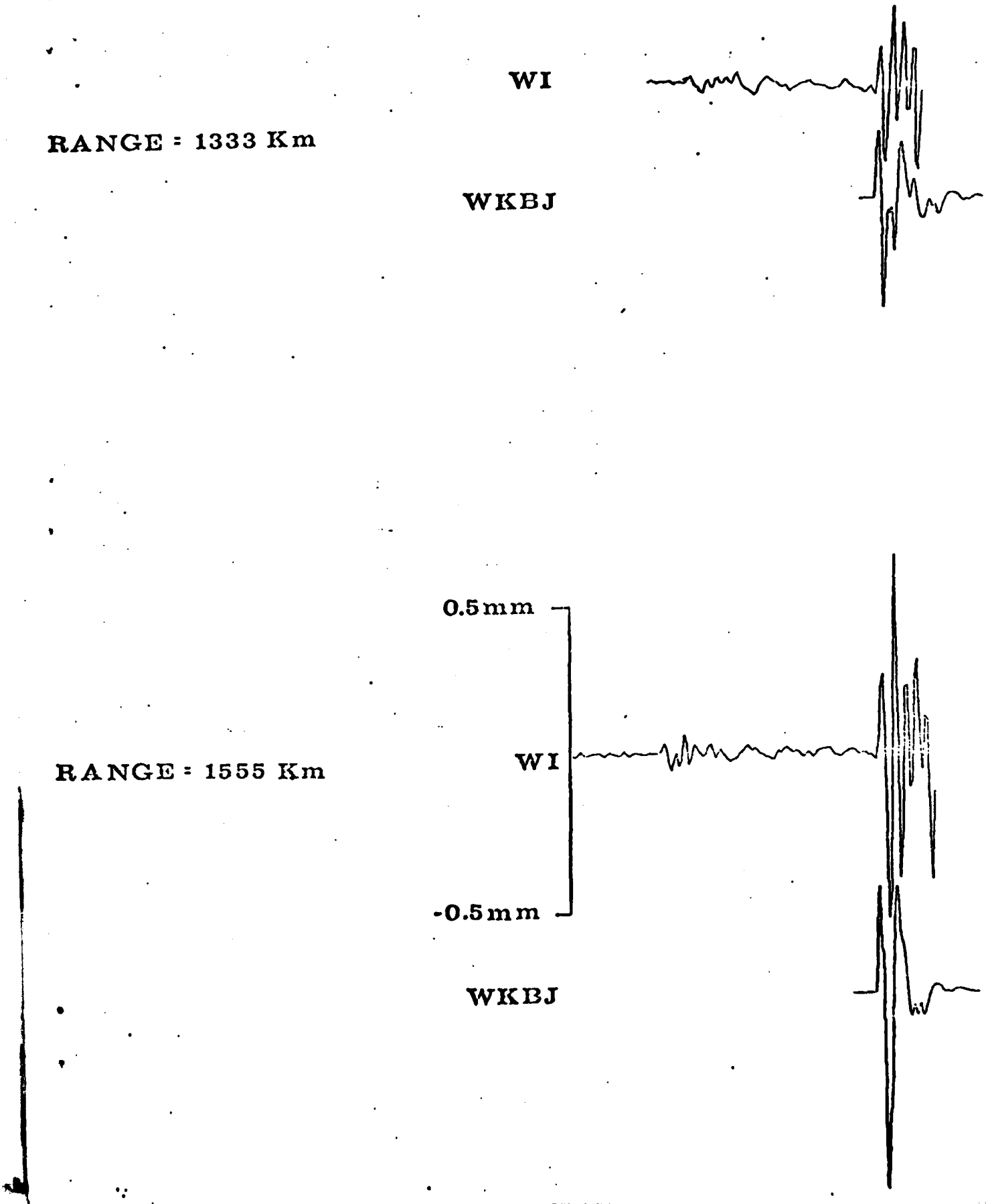
WI
RANGE = 1333 Km
WKBJ
0.5mm
WI
RANGE = 1555 Km
-0.5mm
WKBJ

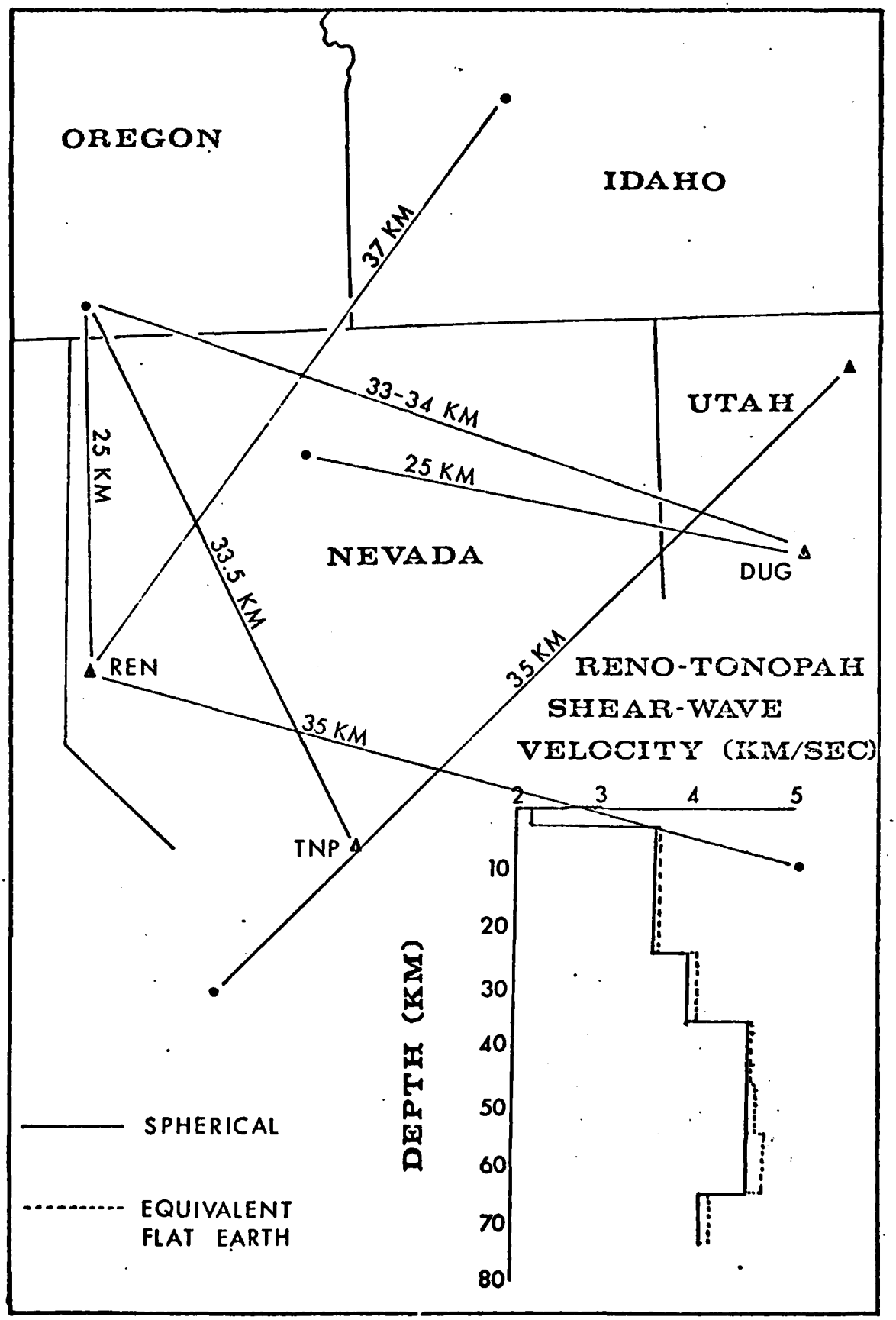
OREGON
IDAHO
UTAH
NEVADA
37 KM
33-34 KM
25 KM
25 KM
33.5 KM
35 KM
35 KM
DUG
REN
TNP
RENO-TONOPAH
SHEAR-WAVE
VELOCITY (KM/SEC)
2
3
4
5
10
20
30
40
50
60
70
80
DEPTH (KM)
SPHERICAL
EQUIVALENT
FLAT EARTH